

Electronic Supplementary Information for

Effect of Disulfide Loop Length on Mechanochemical

Structural Stability of Macromolecules

Feng Wang,^{1,2} and Charles E. Diesendruck^{1,3}

¹ Schulich Faculty of Chemistry, Technion – Israel Institute of Technology, Haifa, 32000, Israel.

² School of Chemical Engineering, Changchun University of Technology, Changchun 130012, P. R. China.

³ Russell-Berrie Nanotechnology Institute; Technion – Israel Institute of Technology, Haifa, 32000, Israel.

Table of Contents

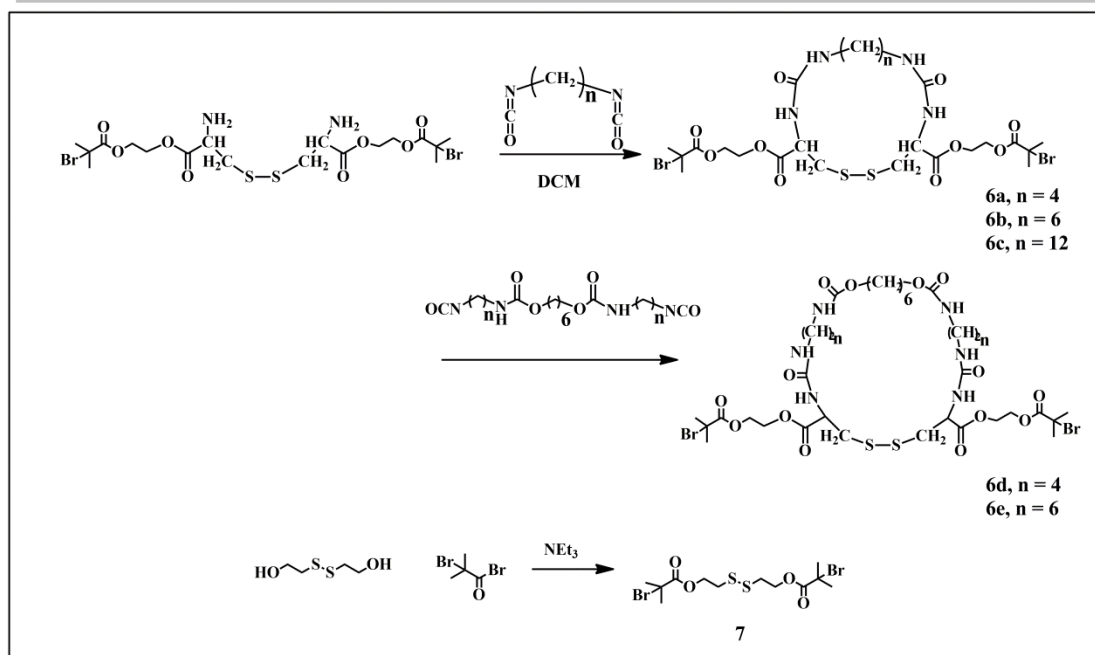
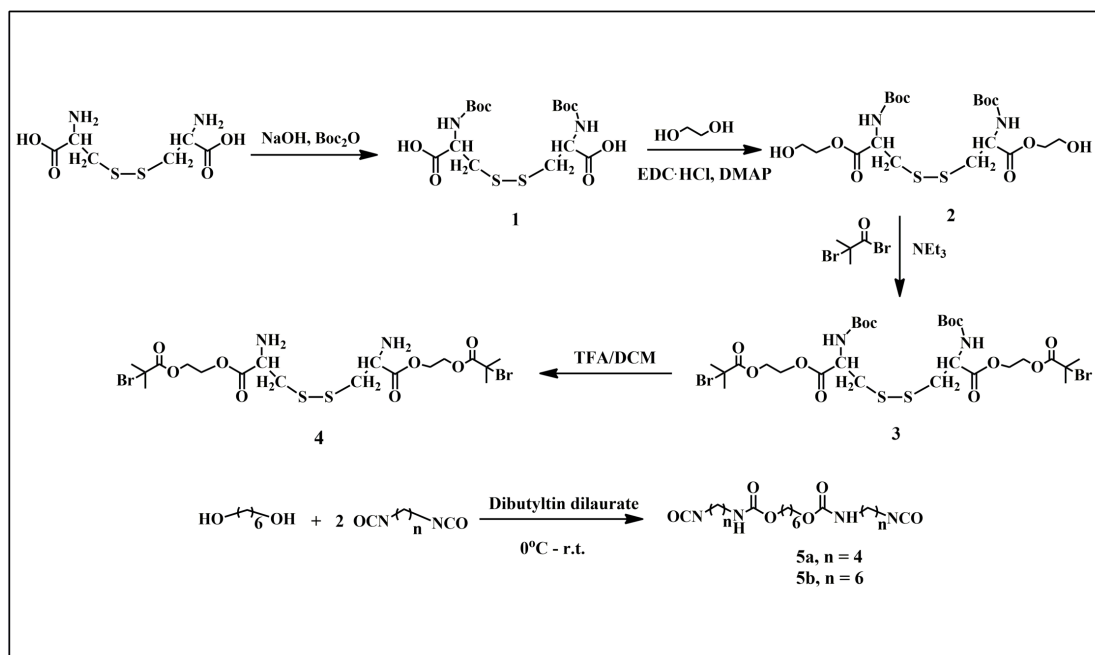
I. General experimental details.....	S3
II. Synthetic details.....	S4
III. General procedure for the synthesis of loop and linear PMA.....	S10
IV. General procedure for sonication experiments.....	S10
V. NMR spectra.....	S11
VI. Kinetic GPC curves.....	S24
VII. Statistic analysis.....	S30
VIII. CoGEF analysis.....	S31
IX. References.....	S36

I. General experimental details

α -bromoisobutyryl bromide was provided by Chemada Fine Chemicals and used as received. All other chemicals were purchased from commercial sources and used, unless specified, as received. MA was purified by passing through basic alumina to remove the inhibitor and kept at 0 °C under argon. Tetrahydrofuran, dichloromethane, dimethylsulfoxide were purified as described by Williams et al.¹ All reactions were carried out in heat-gun-dried glassware under argon atmosphere using standard *Schlenk* techniques.

All ¹H and ¹³C NMR spectra were recorded using an AVANCE II 400 MHz or an AVANCE 300 MHz Bruker spectrometer at the Technion NMR facilities. Proton chemical shifts are expressed in parts per million (ppm, δ scale) and are referenced to tetramethylsilane ((CH₃)₄Si, 0.00 ppm) or residual proton in the solvent (CHCl₃, 7.26 ppm and DMSO-*d*₅, 2.50 ppm). Data are presented as follows: chemical shift, multiplicity (s = singlet, d = doublet, t = triplet, q = quartet, dd = double doublet, m = multiplet and /or multiple resonances, br = broad peak), integration, and coupling constant (*J*) in hertz. Carbon chemical shifts are expressed in parts per million (ppm, δ scale) and referenced to the carbon resonance of the NMR solvents (CDCl₃, 77.16 ppm or DMSO-*d*₆, 39.52 ppm). HRMS ESI (*m/z*) spectra were recorded on Waters LCT Premier Mass Spectrometer, Waters ACQITY UPLC System: ESI+, MeCN : H₂O (70 : 30) 0.25 mL/min. Gel-Permeation Chromatography (GPC) measurements were performed at a flow rate of 1 ml/min THF at 30 °C on a Thermo HPLC system consisting of a Dionex ultimate 3000 isocratic pump, four in line TSKgel G4000HHR columns and a series of five detectors, Dionex DAD-3000 UV-VIS detector, a Wyatt Dawn Heleos II 8 multi-angle light scattering, including DLS (Wyatt QELS), refractometer (Wyatt Optilab-rEX) and viscometer (Wyatt Viscostar II). Data analysis was performed using the ASTRA software from Wyatt. Sonication experiments were performed using Vibra Cell VCX 500 liquid processor under N₂. Thin layer chromatography was carried out on Dynamic Adsorbents silica gel TLC (F-254, 250 μ m). Flash column chromatography was conducted with silica gel 60 (230-400 mesh) from Merck.

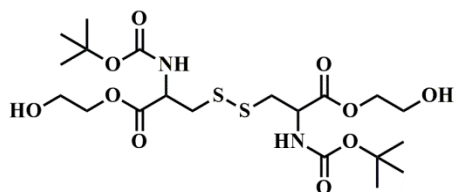
II. Synthetic details



1. L-Boc-cystine (1)

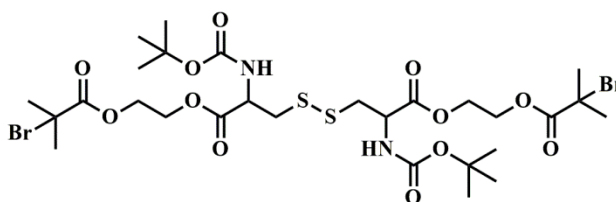
L-Boc-cystine was synthesized as described by Yang et al². ¹H and ¹³C NMR spectra are in accordance with those reported in the literature.

2. Compound 2



A round bottom flask was charged with **1** (4.0 g, 9.08 mmol, 1 equiv), 4-dimethylaminopyridine (DMAP) (0.67 g, 5.45 mmol, 0.6 equiv) and ethylene glycol (25 mL). After a clear solution was obtained, a solution of N-(3-dimethylaminopropyl)-N'-ethylcarbodiimide hydrochloride (EDC) (4.35 g, 22.70 mmol, 2.5 equiv) in ethylene glycol (5.0 mL) was added. The mixture was stirred overnight. Water (100 mL) was then added and the mixture was extracted with CH₂Cl₂ (3 × 50 mL). The combined organic phase was dried over MgSO₄ and filtered. The product was purified through silica chromatography (hexane 1 : 2 ethyl acetate). The solvent was removed under vacuum to give **2** (2.1 g, 41.6% yield) as a colorless oil. ¹H NMR (400 MHz, DMSO-*d*₆) δ 7.38 (dd, *J* = 16.9, 8.3 Hz, 2H, Boc-NH-), 4.80 (t, *J* = 4.7 Hz, 2H, -OH), 4.39-4.21 (m, 2H, -CH₂CH-), 4.12-4.03 (m, 4H, -COOCH₂-), 3.61-3.52 (m, 4H, -CH₂OH), 3.20-2.84 (m, 4H, -SCH₂-), 1.38 (s, 18H, -CH₃). ¹³C NMR (100 MHz, CDCl₃) δ 171.17, 155.68, 80.87, 67.53, 60.54, 53.19, 41.33, 28.47. HRMS (ESI) *m/z*: 551.1722 (calcd C₂₀H₃₆N₂O₁₀S₂Na⁺, 551.1709).

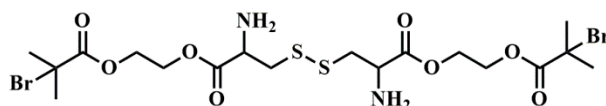
3. Compound 3



Compound **2** (0.50 g, 0.95 mmol, 1 equiv) and triethylamine (0.40 ml, 2.84 mmol, 3 equiv) were dissolved in THF (20 mL) under argon and cooled in an ice bath. Then, a solution of 2-bromo-2-methylpropionyl bromide (0.54g, 2.36mmol, 2.5 equiv) in THF (5 mL) was added dropwise over 30 min. The reaction mixture was allowed to warm to room temperature and stirred overnight. The insoluble salts were removed via filtration and washed with THF (50 mL). The filtrate was concentrated by vacuum

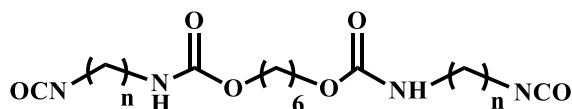
evaporation and the product was purified by silica chromatography (hexane 4:1 ethyl acetate) to afford **3** (0.68 g, yield 86.7%) as yellowish oil. ^1H NMR (400 MHz, CDCl_3) δ 5.39 (d, $J = 7.3$ Hz, 2H, Boc-NH-), 4.73-4.56 (m, 2H, $-\text{CH}_2\text{CH}-$), 4.41 (br s, 8H, $-\text{OCH}_2\text{CH}_2\text{OH}$), 3.43-3.07 (m, 4H, $-\text{SCH}_2-$), 1.94 (s, 12H, $-\text{C}(\text{CH}_3)_2\text{Br}$), 1.45 (s, 18H, $-\text{C}(\text{CH}_3)_3$). ^{13}C NMR (100 MHz, CDCl_3) δ 171.53, 170.50, 155.10, 80.44, 63.31, 63.05, 55.58, 53.07, 41.22, 30.74, 28.47. HRMS (ESI) m/z : 847.0750 (calcd $\text{C}_{28}\text{H}_{46}\text{N}_2\text{O}_{12}\text{S}_2\text{Br}_2\text{Na}^+$, 847.0757).

4. Compound 4



Compound **3** (0.50 g, 0.60 mmol, 1 equiv) was dissolved in neat trifluoroacetic acid (TFA) (1.80 mL, 24.0 mmol, 40 equiv). The mixture was stirred for 3 h and the TFA was evaporated, affording thick, red oil. A solution of saturated NaHCO_3 (10 mL) was added to quench any remaining TFA, until the pH reached 8-9. The solution was then extracted with EtOAc (3×50 mL), and the combined organic layers were dried over MgSO_4 , filtered and evaporated to afford **4** (0.35g, yield 92.1%). ^1H NMR (300 MHz, CDCl_3) δ 4.41 (br s, 8H, $-\text{OCH}_2\text{CH}_2\text{OH}$), 3.96-3.82 (m, 2H, $-\text{CH}_2\text{CH}-$), 3.40-2.88 (m, 4H, $-\text{SCH}_2-$), 1.93 (s, 12H, $-\text{C}(\text{CH}_3)_2\text{Br}$). ^{13}C NMR (100 MHz, CDCl_3) δ 173.31, 171.54, 63.37, 62.79, 55.59, 53.71, 43.20, 30.76. HRMS (ESI) m/z : 624.9880 (calcd $\text{C}_{18}\text{H}_{31}\text{N}_2\text{O}_8\text{S}_2\text{Br}_2^+$, 624.9889).

5. Compounds 5a,b



5a, n = 4

5b, n = 6

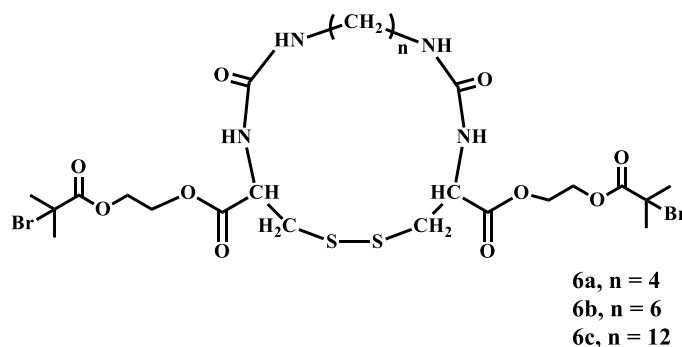
1,6-hexanediol (0.05 g, 0.42 mmol) in anhydrous diethyl ether (6 mL) was added dropwise to a solution of the corresponding diisocyanate (10 equiv) in anhydrous diethyl ether (10 mL) at 0 °C. Then, 4 drops of dibutyltin dilaurate were added. The

reaction mixture was kept at 0 °C for 1 h and further stirred at room temperature for 3 h. The product precipitated as a white solid, which was collected by filtration and dried under vacuum.

5a (0.14 g, yield 85.0%). ¹H NMR (400 MHz, DMSO-*d*₆) δ 7.19-6.94 (m, 2H, -NH-), 3.92 (t, *J* = 6.3 Hz, 4H, -COOCH₂-), 3.35 (t, *J* = 6.4 Hz, 4H, OCNCH₂-), 2.98 (m, 4H, -CH₂NH-), 1.59-1.47 (m, 8H, -COOCH₂(CH₂)₄CH₂OOC-), 1.48-1.39 (m, 4H, -OCNCH₂CH₂-), 1.37-1.22 (m, 4H, -CH₂CH₂NH-). ¹³C NMR (100 MHz, DMSO-*d*₆) δ 156.39, 121.53, 63.51, 42.31 (2C), 28.67, 27.92, 26.53, 25.12. HRMS (ESI) *m/z*: 421.2057 (calcd C₁₈H₃₀N₄O₆Na⁺, 421.2063).

5b (0.18 g, yield 90.3%). ¹H NMR (400 MHz, DMSO) δ 7.03, 5.71 (m, 2H, -NH-), 3.90 (t, *J* = 6.2 Hz, 4H, -COOCH₂-), 3.44-3.23 (t, 4H, *J* = 6.4 Hz, 4H, OCNCH₂-), 3.04-2.83 (m, 4H, -CH₂NH-), 1.63-1.10 (m, 24H, -COOCH₂(CH₂)₄CH₂OOC-, -OCNCH₂(CH₂)₄CH₂NH-). ¹³C NMR (151 MHz, DMSO-*d*₆, 90 °C) δ 155.85, 121.33, 63.08, 42.09, 30.19, 29.54, 28.95, 28.23, 25.49, 25.20, 24.63. HRMS (ESI) *m/z*: 477.2682, (calcd C₂₂H₃₈N₄O₆Na⁺, 477.2689).

6. Compounds 6a-c



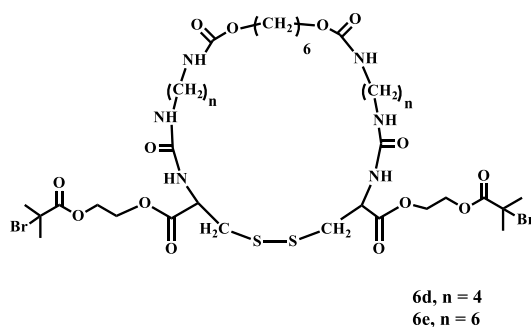
A solution of the corresponding diisocyanate (0.59 mmol) in anhydrous CH₂Cl₂ (40 mL) was added dropwise over a period of 30 - 40 min to a well-stirred and ice-cooled solution of the freshly generated compound **4** (0.37 g, 0.59 mmol) in anhydrous CH₂Cl₂ (170 mL). The reaction mixture was then stirred at room temperature for 72 h. The solvent was evaporated and the residue was separated by silica chromatography (dichloromethane 40: 1 methanol), affording the corresponding product as a white solid.

6a (0.16 g, yield 35.6%). ^1H NMR (400 MHz, DMSO) δ 6.35 (dd, $J = 20.1, 8.1$ Hz, 2H, -CHNH-), 6.28-6.08 (m, 2H, -CONHCH₂-), 4.70-4.44 (m, 2H, -CHNH-), 4.32 (br s, 8H, -OCH₂CH₂O-), 3.27-2.62 (m, 8H, -CH₂NH-, -SCH₂-), 1.88 (s, 12H, -C(CH₃)₂Br), 1.65-0.96 (m, 4H, -NHCH₂(CH₂)₂CH₂NH-). ^{13}C NMR (100 MHz, CDCl₃ + CD₃OD) δ 171.65, 171.10, 158.35, 63.57, 62.90, 55.45, 52.59, 42.24, 39.79, 30.65, 27.25. HRMS (ESI) m/z : 767.0480 (calcd C₂₄H₃₉N₄O₁₀S₂Br₂⁺, 767.0454).

6b (0.49g, yield 42.1%). ^1H NMR (400 MHz, DMSO-*d*₆) δ 6.47-6.32 (m, 2H, -CHNH-), 6.35 (dd, $J = 20.1, 8.1$ Hz, 2H), 6.22-5.96 (m, 2H, -CONHCH₂-), 4.68-4.48 (m, 2H, -CHNH-), 4.34 (br s, 8H, -OCH₂CH₂O-), 3.15-2.83 (m, 4H, -SCH₂-), 3.28-2.60 (m, 8H, -CH₂NH-, -SCH₂-), 1.89 (s, 12H, -C(CH₃)₂Br), 1.38-1.18 (m, 8H, -NHCH₂(CH₂)₄CH₂NH-). ^{13}C NMR (100 MHz, CDCl₃ + CD₃OD) δ 171.54, 171.08, 158.17, 63.28, 62.86, 55.36, 52.39, 42.01, 37.85, 30.42, 29.26, 24.98, 23.70. HRMS (ESI) m/z : 795.0754 (calcd C₂₆H₄₃N₄O₁₀S₂Br₂⁺, 795.0767)

6c (0.69g, yield 36.6%). ^1H NMR (400 MHz, DMSO-*d*₆) δ 6.33 (m, 2H, dd, $J = 20.1, 8.1$ Hz, -CHNH-), 6.17-6.05 (m, 2H, -CONHCH₂-), 4.61-4.42 (m, 2H, -CHNH-), 4.40-4.22 (br s, 8H, -OCH₂CH₂O-), 3.27-2.74 (m, 8H, -CH₂NH-, -SCH₂-), 1.95-1.84 (m, 12H, -C(CH₃)₂Br), 1.43-1.12 (m, 20H, -NHCH₂(CH₂)₁₀CH₂NH-). ^{13}C NMR (100 MHz, CDCl₃ + CD₃OD) δ 171.53, 171.16, 158.18, 63.26, 62.67, 55.37, 52.24, 41.36, 39.74, 30.41, 29.37, 27.43, 27.14, 26.86, 25.65. HRMS (ESI) m/z : 877.1750 (calcd C₃₂H₅₅N₄O₁₀S₂Br₂⁺, 877.1726).

7. Compound 6d,e



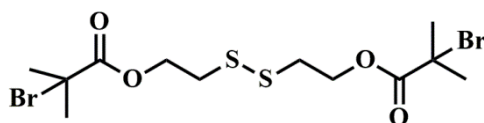
A solution of compound **5a** or **5b** (0.72 mmol) in a mixture of anhydrous DMSO (5 mL) and anhydrous CH₂Cl₂ (40 mL) was added dropwise over a period of 30 - 40

min to a well-stirred and ice-cooled solution of the freshly generated compound **4** (0.45 g, 0.72 mmol) in anhydrous CH₂Cl₂ (200 mL). The mixture was then left stirred at room temperature for 72 h. The solvents was evaporated and the product was purified by silica chromatography (dichloromethane 40 : 1 methanol), affording the corresponding product as white solid.

6d (0.15g, yield 20.1%). ¹H NMR (400 MHz, DMSO-*d*₆) δ 7.04 (t, *J* = 5.4 Hz, 2H, -NHCOO-), 6.34 (d, *J* = 8.1 Hz, 2H, -CHNH-), 6.15 (t, *J* = 5.5 Hz, 2H, -CH₂NHCONH-), 4.61-4.43 (m, 2H, -CHNH-), 4.41-4.25 (br s, 8H, -OCH₂CH₂O-), 3.91 (t, *J* = 6.1 Hz, 4H, -OCH₂CH₂O-), 3.13-2.81 (m, 12H, -SCH₂-, -NHCH₂(CH₂)₄CH₂NH-), 1.88 (s, 12H, -C(CH₃)₂Br), 1.61-1.21 (m, 16H, -NHCOOCH₂(CH₂)₄CH₂OOCNH-, -NHCH₂(CH₂)₂CH₂NH-). ¹³C NMR (100 MHz, CDCl₃ + CD₃OD) δ 171.44, 171.03, 158.12, 157.45, 64.23, 63.15, 62.60, 55.24, 52.14, 41.20, 40.04, 39.29, 30.21, 27.96, 27.02, 26.81, 24.73. HRMS (ESI) *m/z*: 1023.2050 (calcd C₃₆H₆₁N₆O₁₄S₂Br₂⁺, 1023.2054).

6e (0.16 g, yield 23.2%). ¹H NMR (300 MHz, DMSO-*d*₆) δ 7.01 (t, *J* = 5.1Hz, 2H, -NHCOO-), 6.35 (d, *J* = 8.3 Hz, 2H, -CHNH-), 6.15 (t, *J* = 5.7 Hz, 2H, -CH₂NHCONH-), 4.64-4.41 (m, 2H, -CHNH-), 4.32 (br s, 8H, -OCH₂CH₂O-), 3.99-2.80 (m, 4H, -OCH₂CH₂O-), 3.15-2.80 (m, 12H, -SCH₂-, -NHCH₂(CH₂)₄CH₂NH-), 1.87 (s, 12H, -C(CH₃)₂Br), 1.57-1.45 (m, 8H, -NHCOOCH₂(CH₂)₄CH₂OOCNH-), 1.42-1.26 (m, 16H, -NHCH₂(CH₂)₄CH₂NH-). ¹³C NMR (100 MHz, CDCl₃ + CD₃OD) δ 171.45, 171.06, 158.06, 157.32, 64.42, 63.17, 62.66, 55.28, 52.12, 41.38, 40.30, 39.55, 30.29, 29.71, 29.47, 28.58, 26.08 (2C), 25.20. HRMS (ESI) *m/z*: 1081.2660 (calcd C₄₀H₆₉N₆O₁₄S₂Br₂⁺, 1081.2659).

8. Bis[2-(2-bromoisobutyryloxy)ethyl] disulfide (BiBS) (**7**)



7 was synthesized according to a literature procedure.^{3,4} ¹H and ¹³C NMR spectra are in accordance with those reported in the literature.⁵

III. General procedure for the synthesis of *loop*-PMAs and *linear*-PMA.

The polymers with different macrocyclic centers were synthesized through SET-LRP.⁵ The procedure described for **1a** was used also for the different initiators.

MA (1.0 mL, 11.10 mmol), solvent (DMSO, 0.5 mL), initiator (**1a**, 5.87 mg, 7.65 μmol), copper wire (diam. 0.5mm, 1 cm length), and ligand (Me₆TREN, 1.0 μL , 3.83 μmol) were added to a 10 mL Schlenk flask under argon in the following order: copper wire, monomer, ligand, solvent and initiator. The flask was immediately sealed and three freeze-pump-thaw cycles were applied to remove dissolved oxygen. The flask was backfilled with argon and allowed to stir in a water bath for 2 h at room temperature. The polymerization was quenched by opening to air, after which THF (10 mL) was added. The polymer solution was filtered through a pad of silica gel and concentrated by evaporation. The polymer was then precipitated in cold methanol, collected and dried under vacuum overnight.

IV. General procedure for sonication experiments.

Polymer (20 mg) was dissolved in THF (20 mL, containing 50 eq. of BHT) and transferred to a Suslick cell, which was placed into collar and screwed on to the probe. A N₂ line was introduced into the cell and N₂ was started to sparged through the system 30 min ahead of the sonication experiment, during which the Suslick cell was placed in a cooling bath (-9 °C). Pulsed ultrasound (1.0 s on, 2.0 s off, 500 watt, 20 kHz, 20% amplitude, 9.55 W cm⁻²) was applied to the system and aliquots of 500 μL were removed at 0, 15, 30, 45, 60, 75, 90, 105 and 120 min. Every sample was filtered through a syringe filter (PTFE, 0.45 μm pore size) and analyzed by GPC.

V. NMR spectra

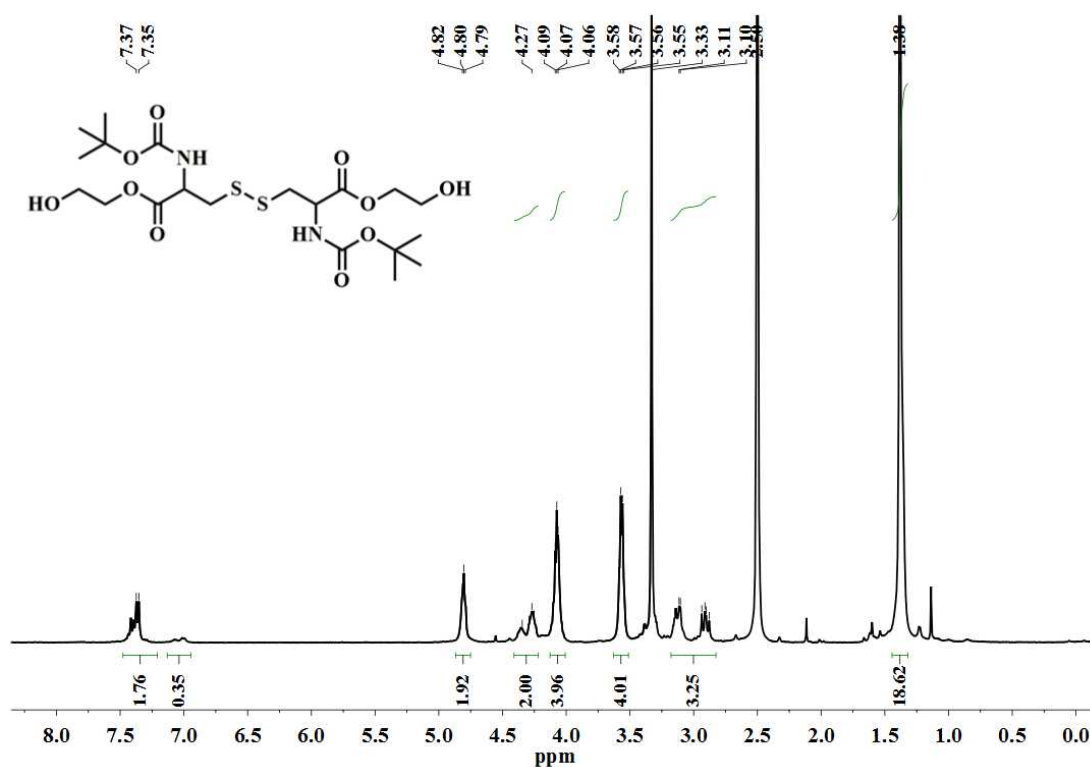


Figure S1. ¹H NMR of compound 2 in DMSO-*d*₆.

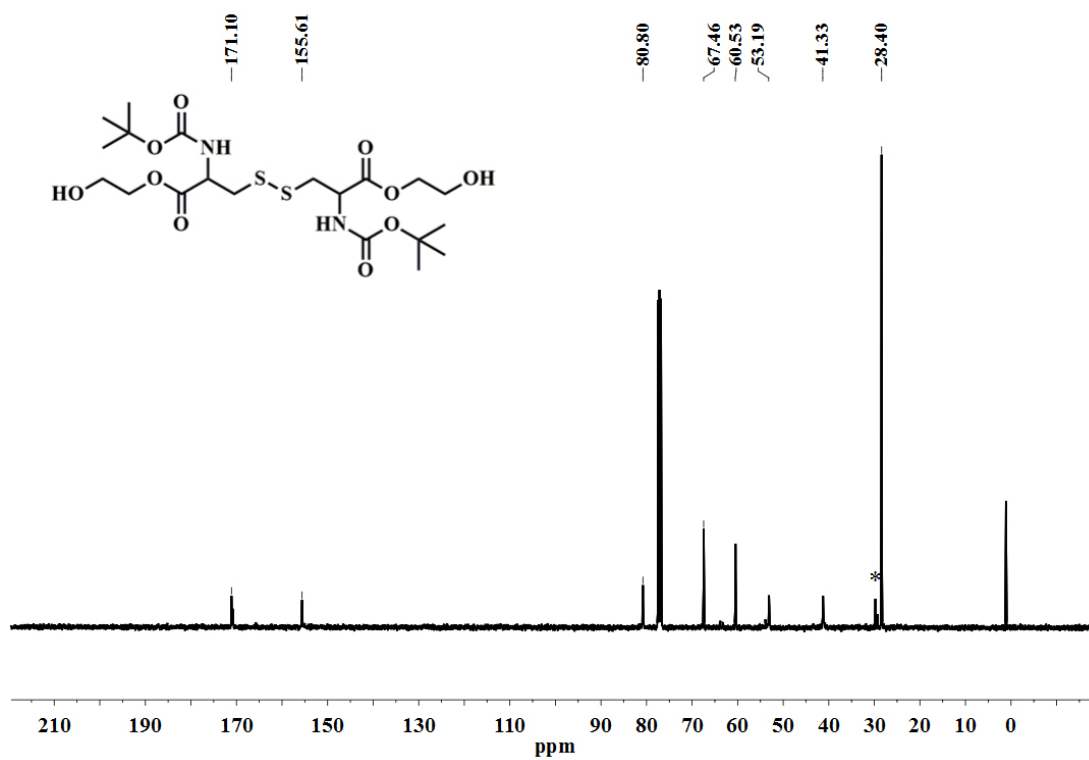


Figure S2. ¹³C NMR of compound 2 in DMSO-*d*₆, *grease.

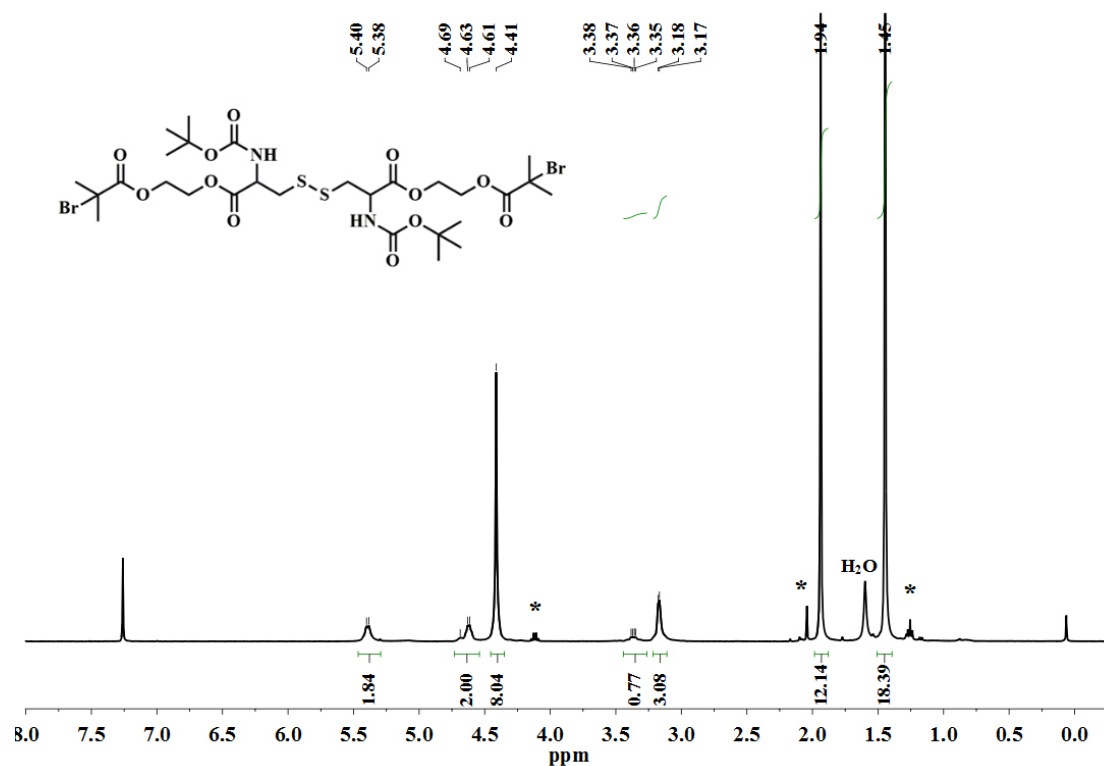


Figure S3. ^1H NMR of compound **3** in CDCl_3 , *ethyl acetate.

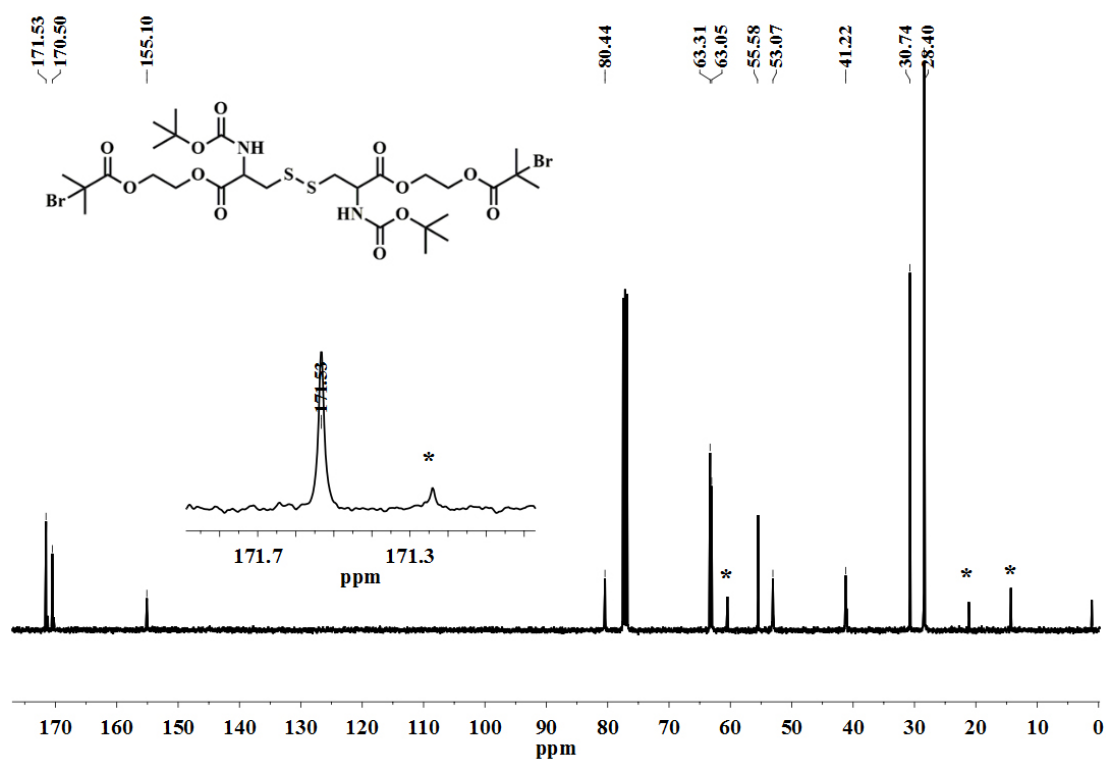


Figure S4. ^{13}C NMR of compound **3** in CDCl_3 , *ethyl acetate.

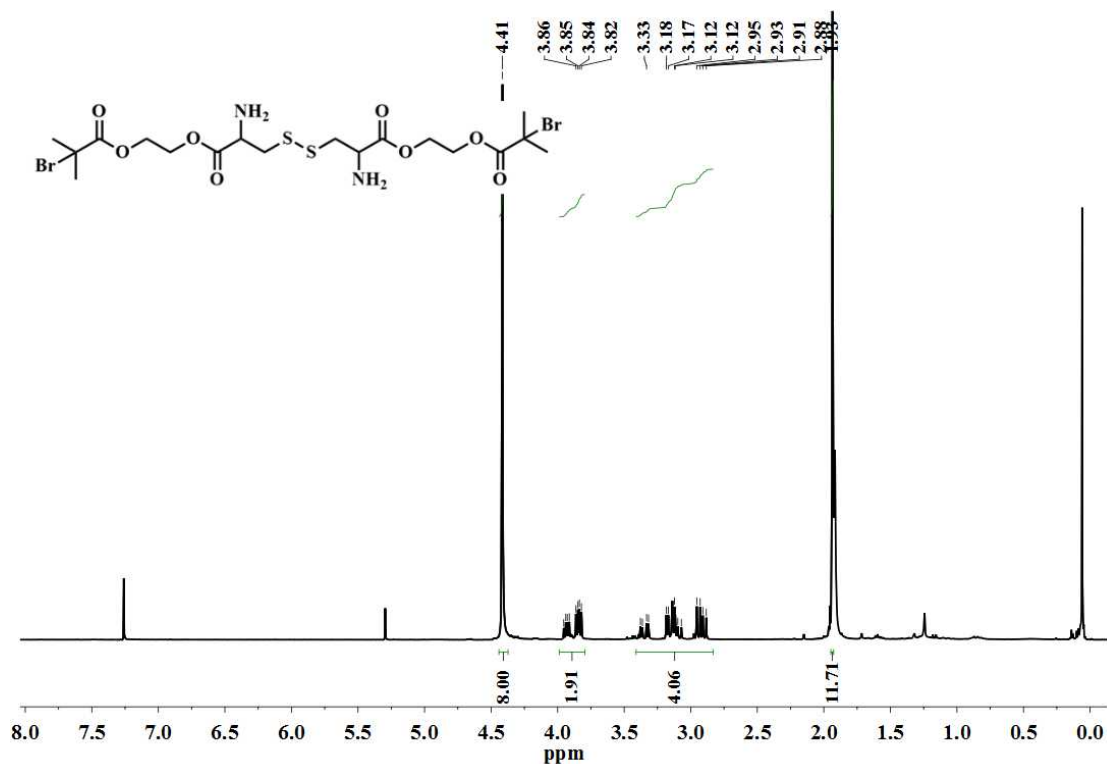


Figure S5. ¹H NMR of compound 4 in CDCl₃.

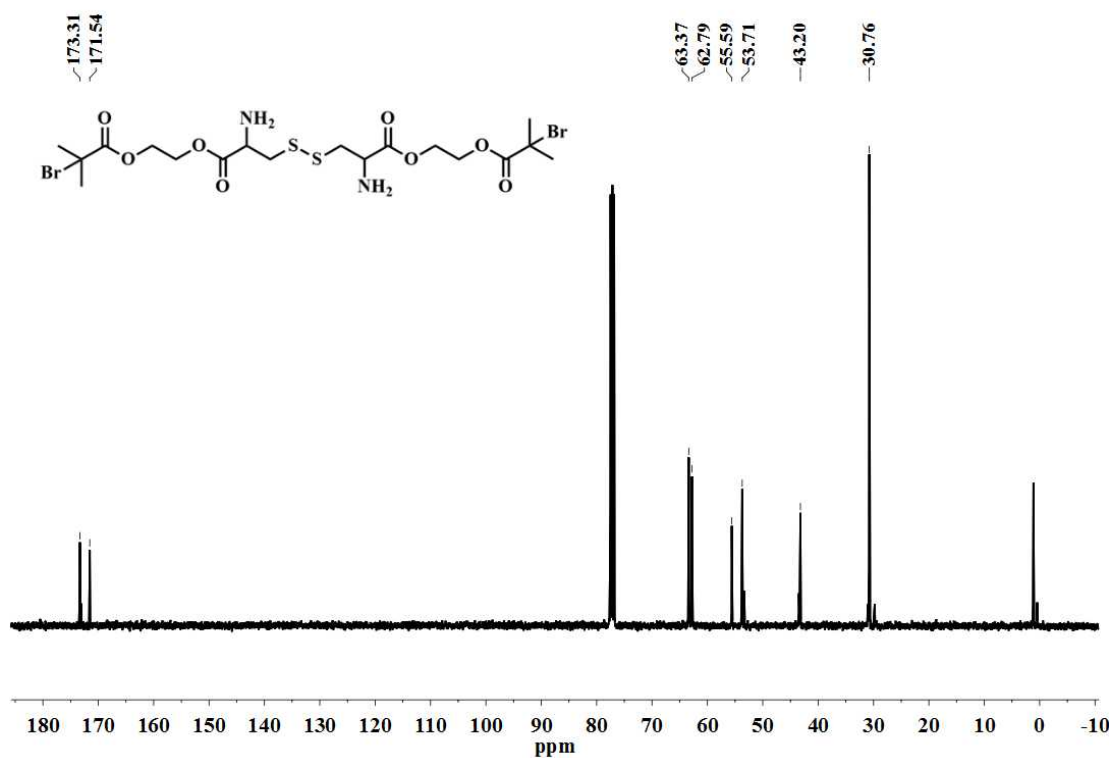


Figure S6. ¹³C NMR of compound 4 in CDCl₃.

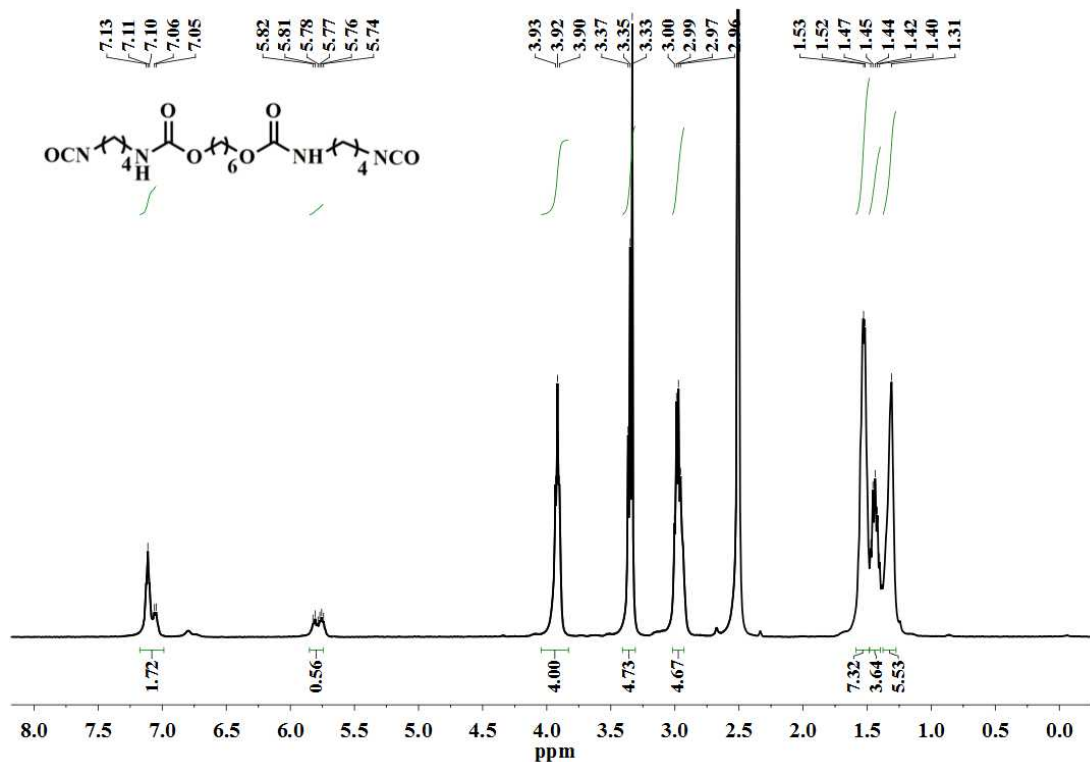


Figure S7. ^1H NMR of compound **5a** in $\text{DMSO-}d_6$.

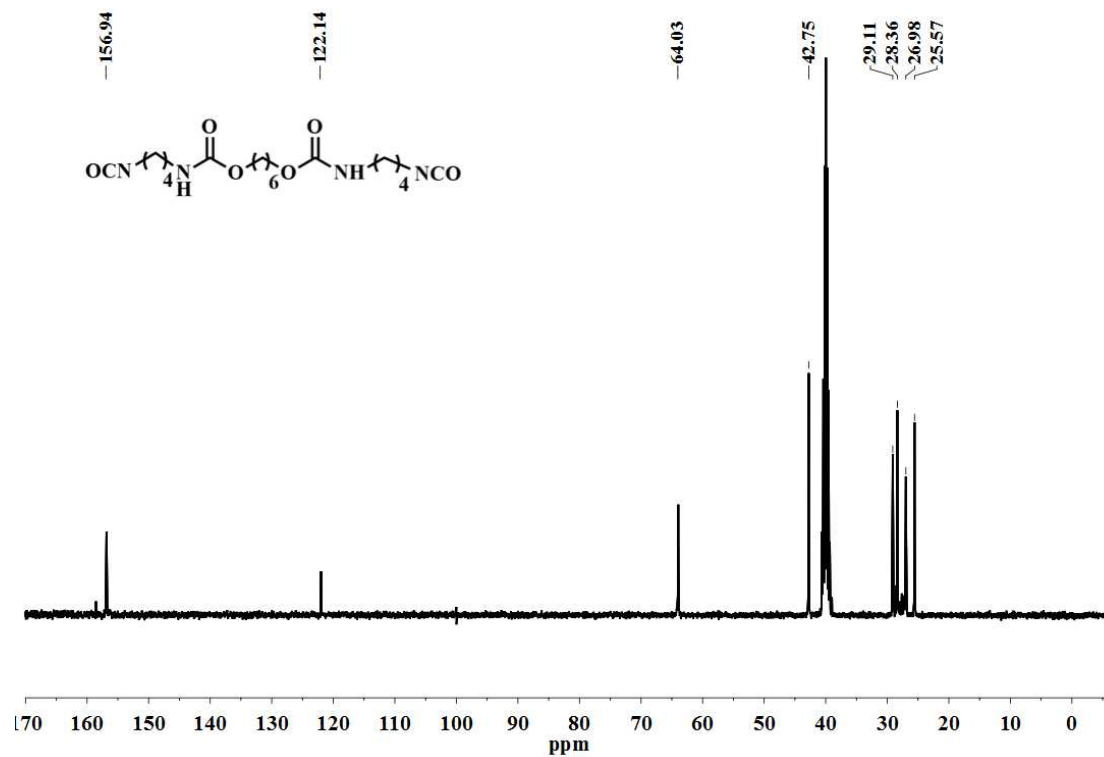


Figure S8. ^{13}C NMR of compound **5a** in $\text{DMSO-}d_6$.

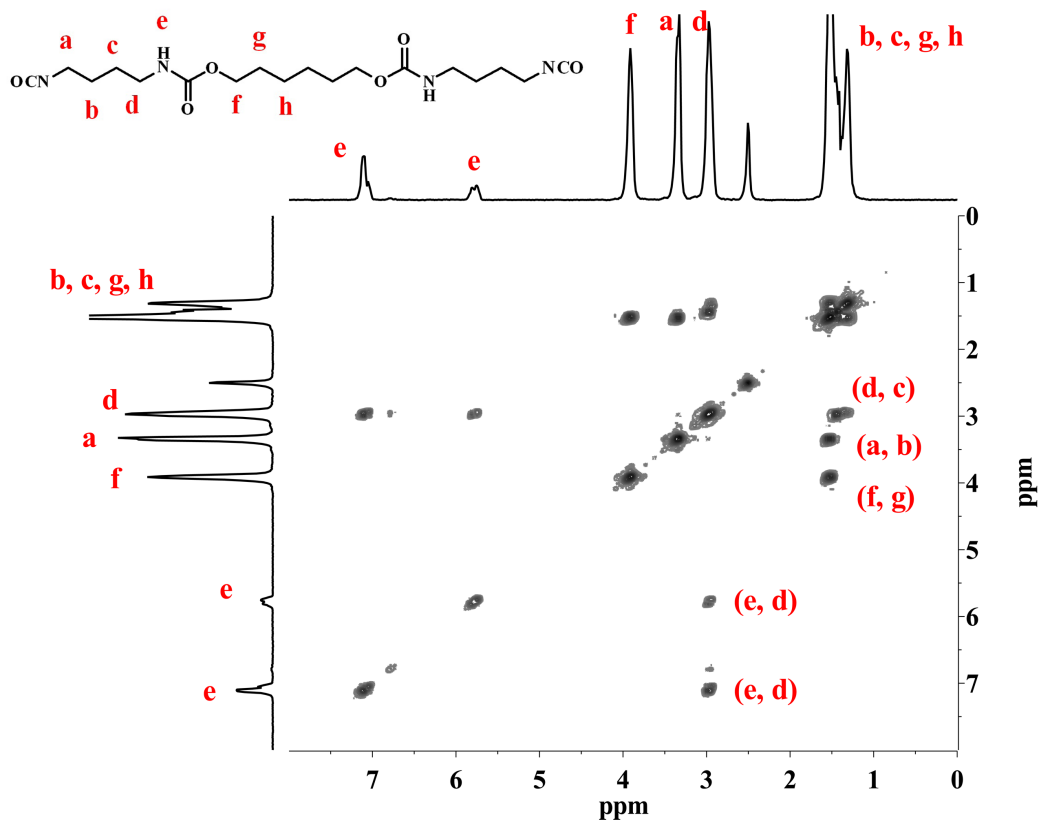


Figure S9. ^1H COSY spectrum of **5a** in $\text{DMSO-}d_6$.

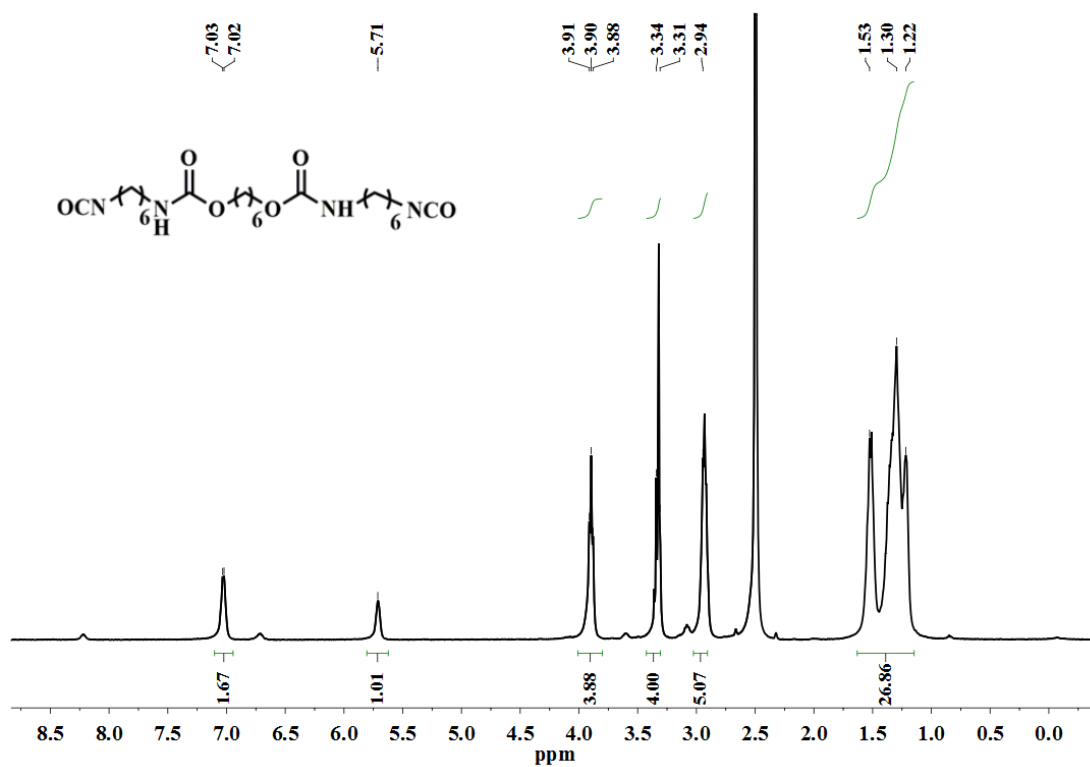


Figure S10. ^1H NMR of compound **5b** in $\text{DMSO-}d_6$.

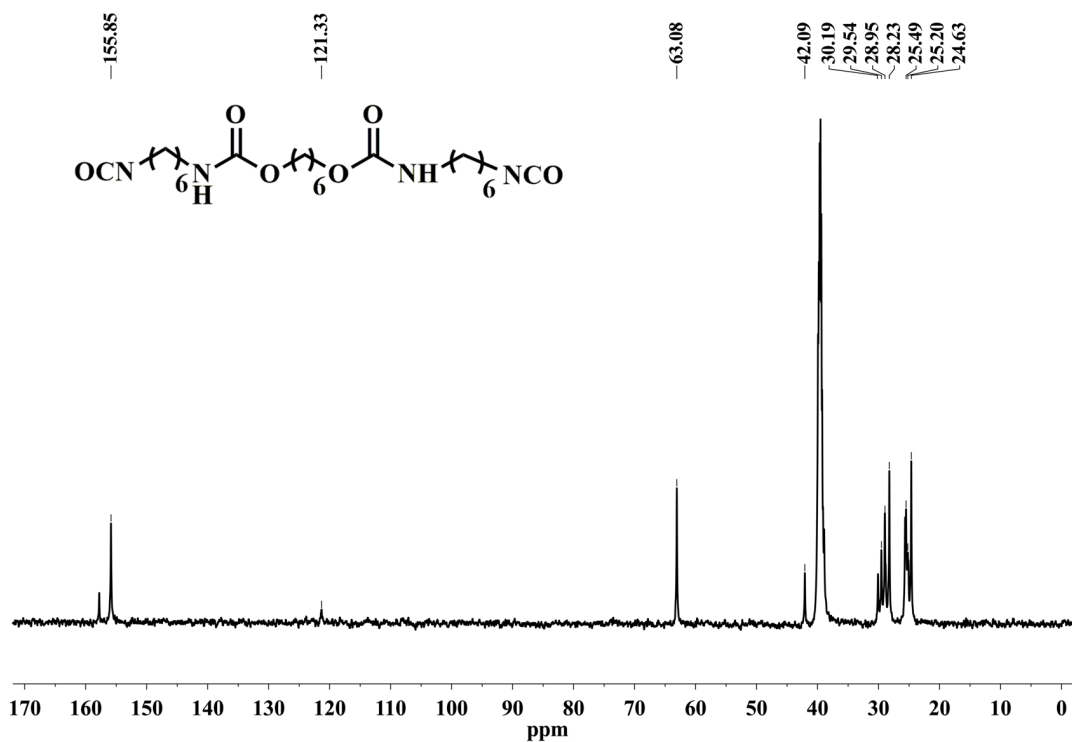


Figure S11. ^{13}C NMR of compound **5b** in $\text{DMSO-}d_6$ at $90\text{ }^\circ\text{C}$.

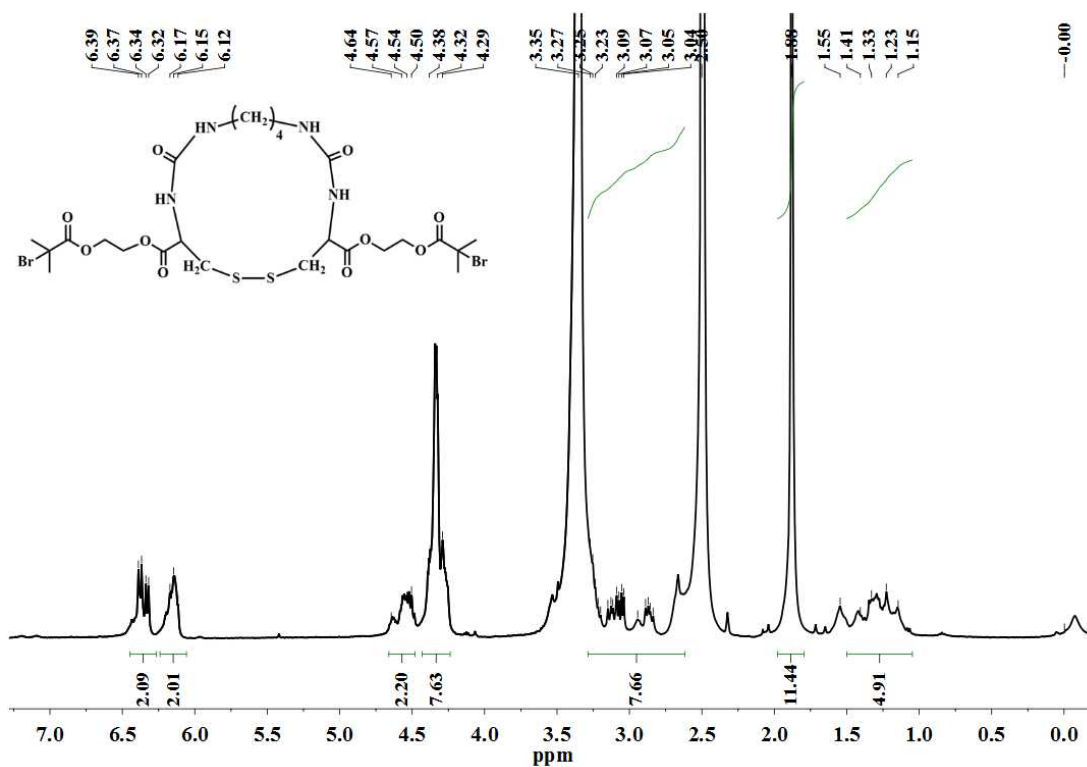


Figure S12. ^1H NMR of compound **6a** in $\text{DMSO-}d_6$.

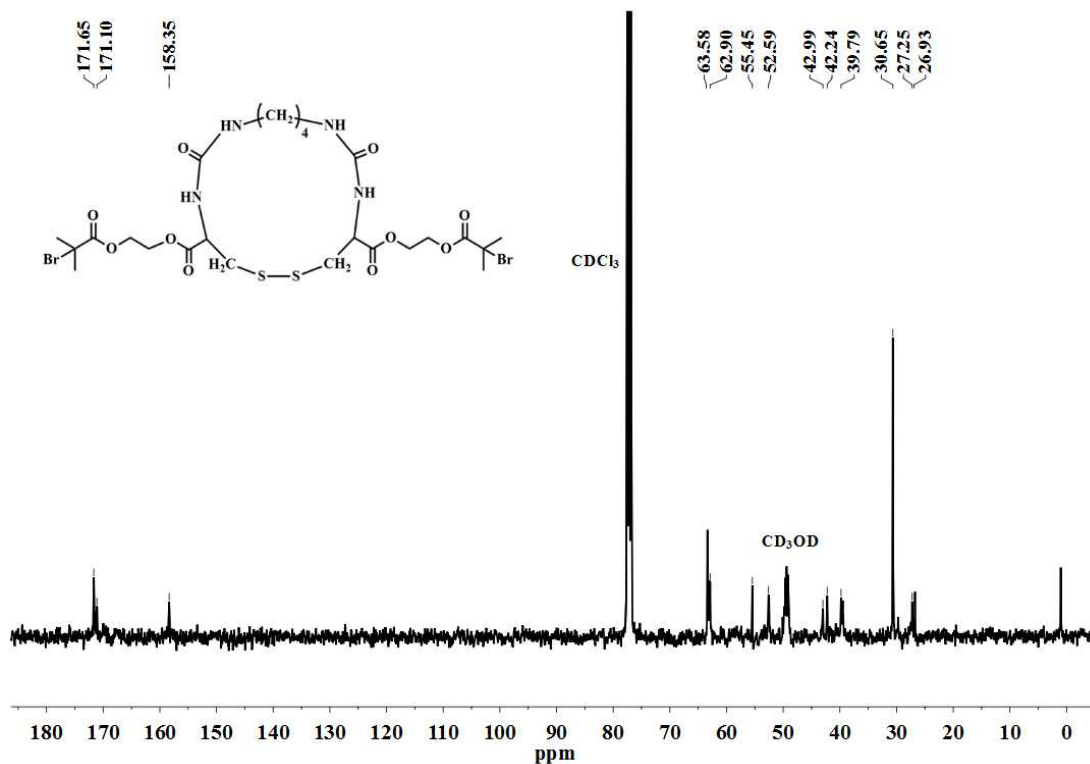


Figure S13. ^{13}C NMR of compound **6a** in $\text{CDCl}_3 + \text{CD}_3\text{OD}$.

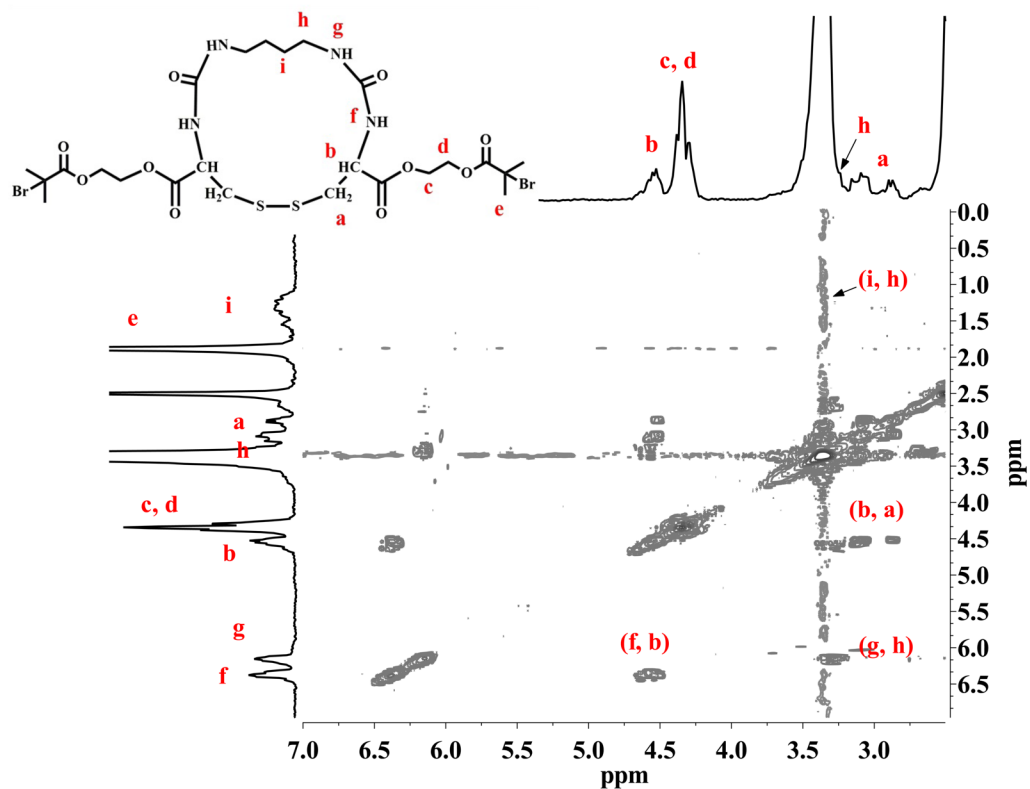


Figure S14. ^1H COSY spectrum of **6a** in $\text{DMSO-}d_6$.

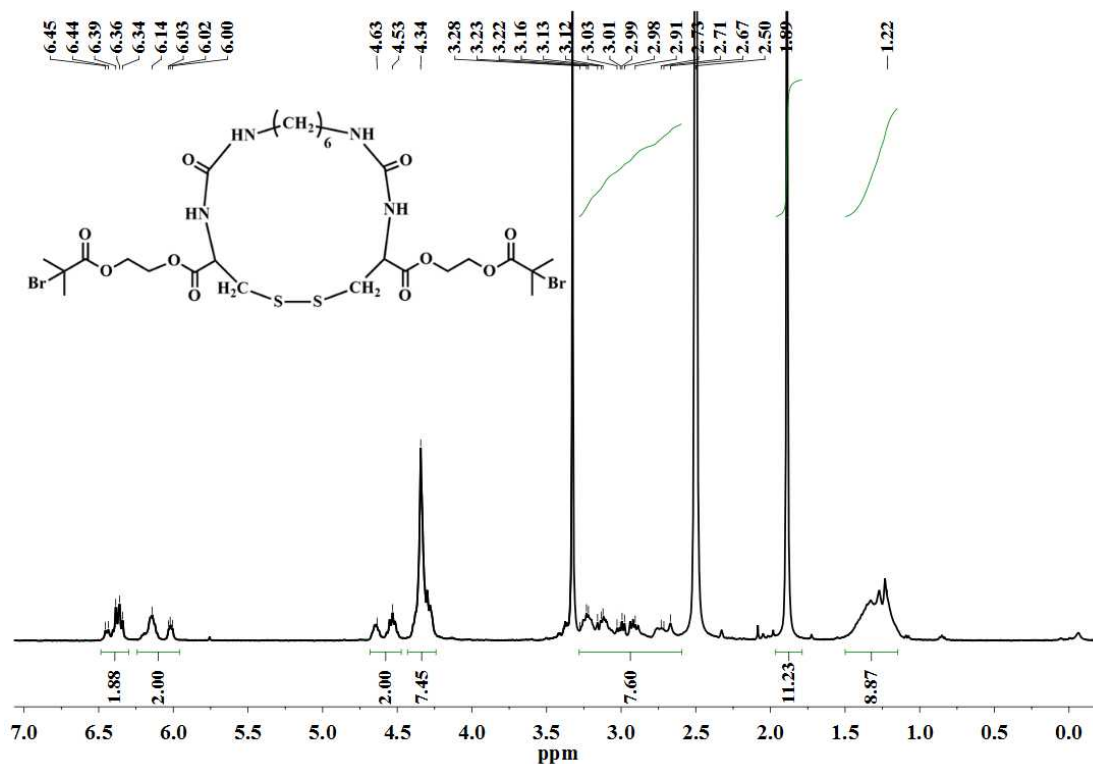


Figure S15. ¹H NMR of compound **6b** in DMSO-*d*₆.

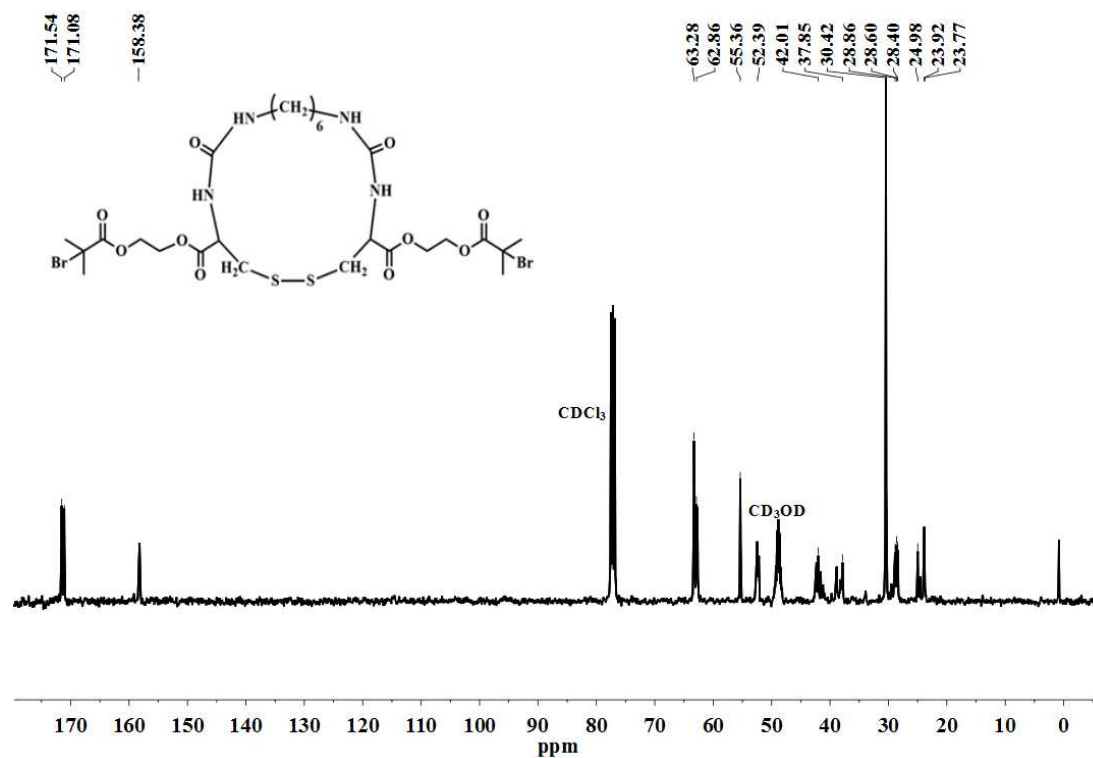


Figure S16. ¹³C NMR of compound **6b** in CDCl₃ + CD₃OD.

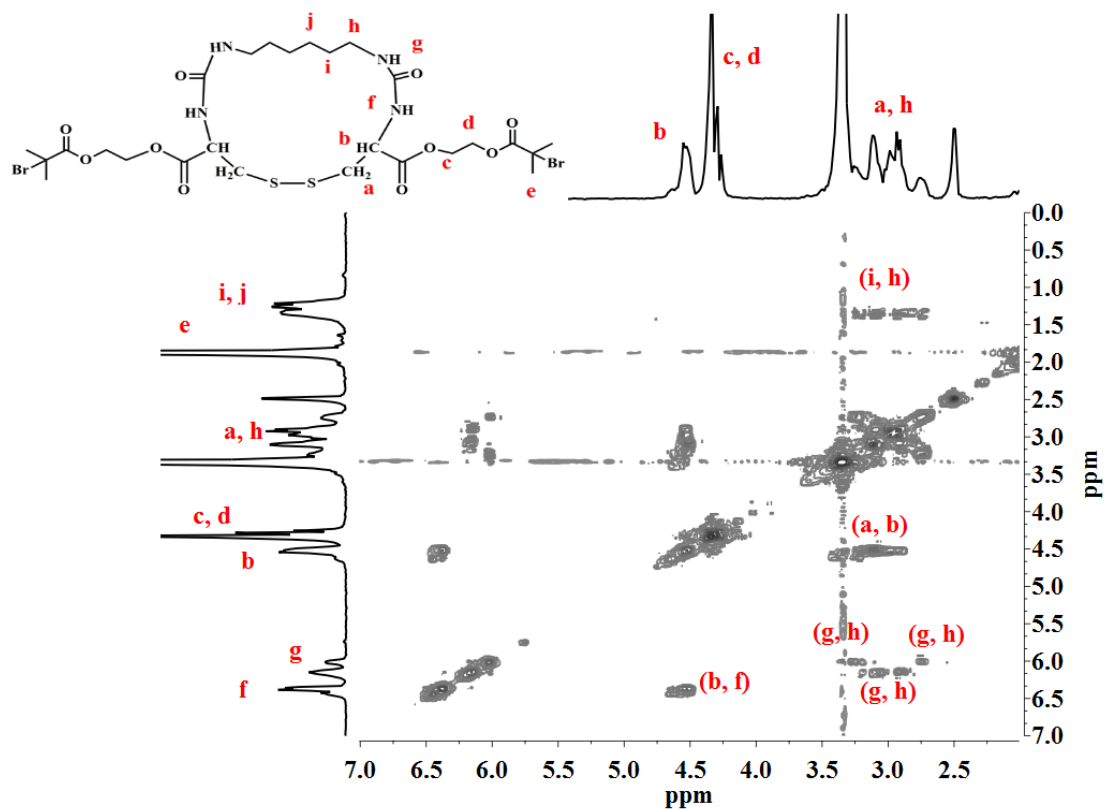


Figure S17. ^1H COSY spectrum of **6b** in $\text{DMSO-}d_6$

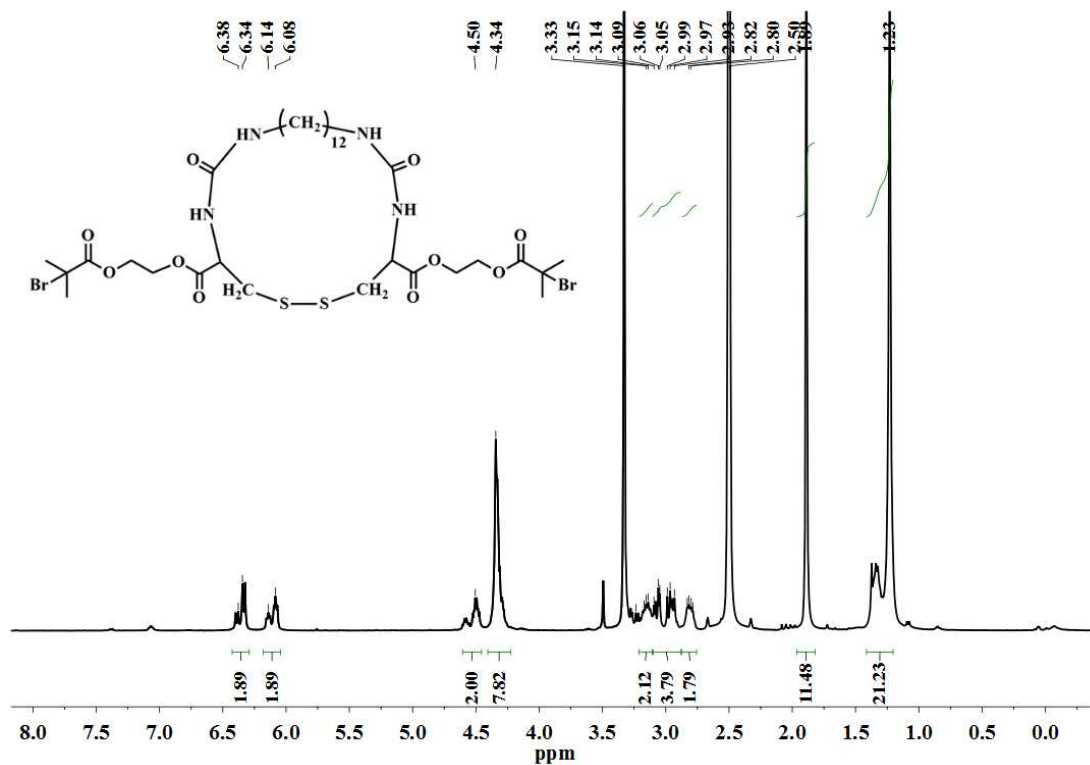


Figure S18. ^1H NMR of compound **6c** in $\text{DMSO-}d_6$.

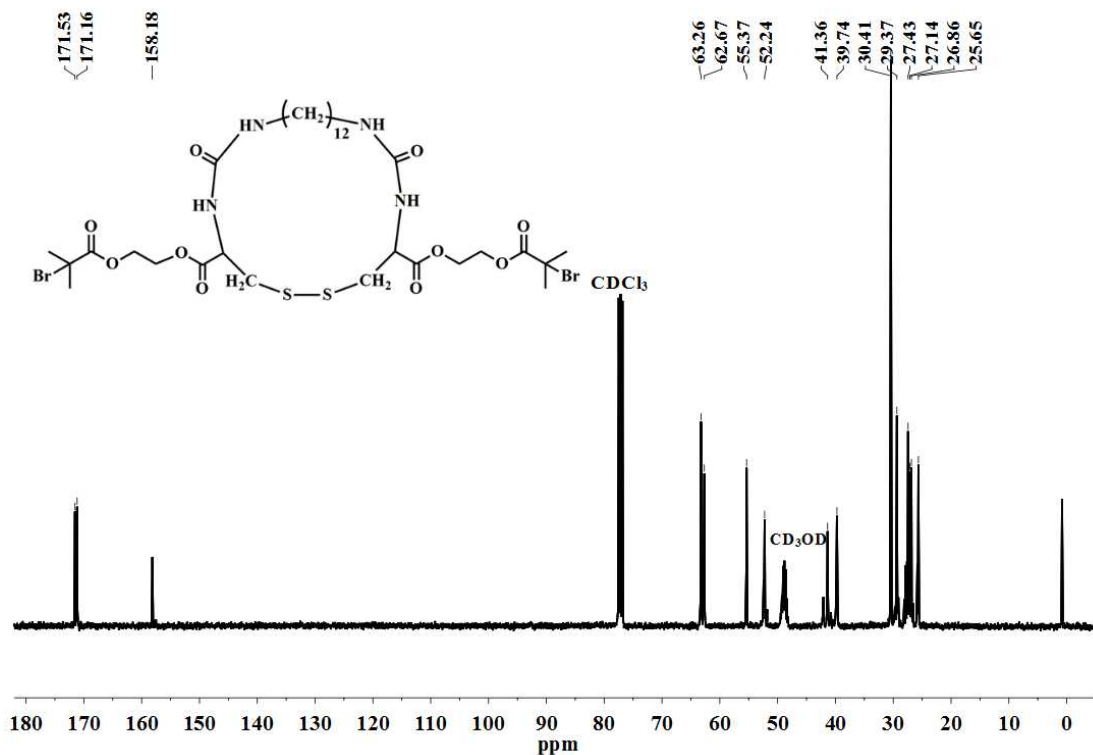


Figure S19. ^{13}C NMR of compound **6c** in $\text{CDCl}_3 + \text{CD}_3\text{OD}$.

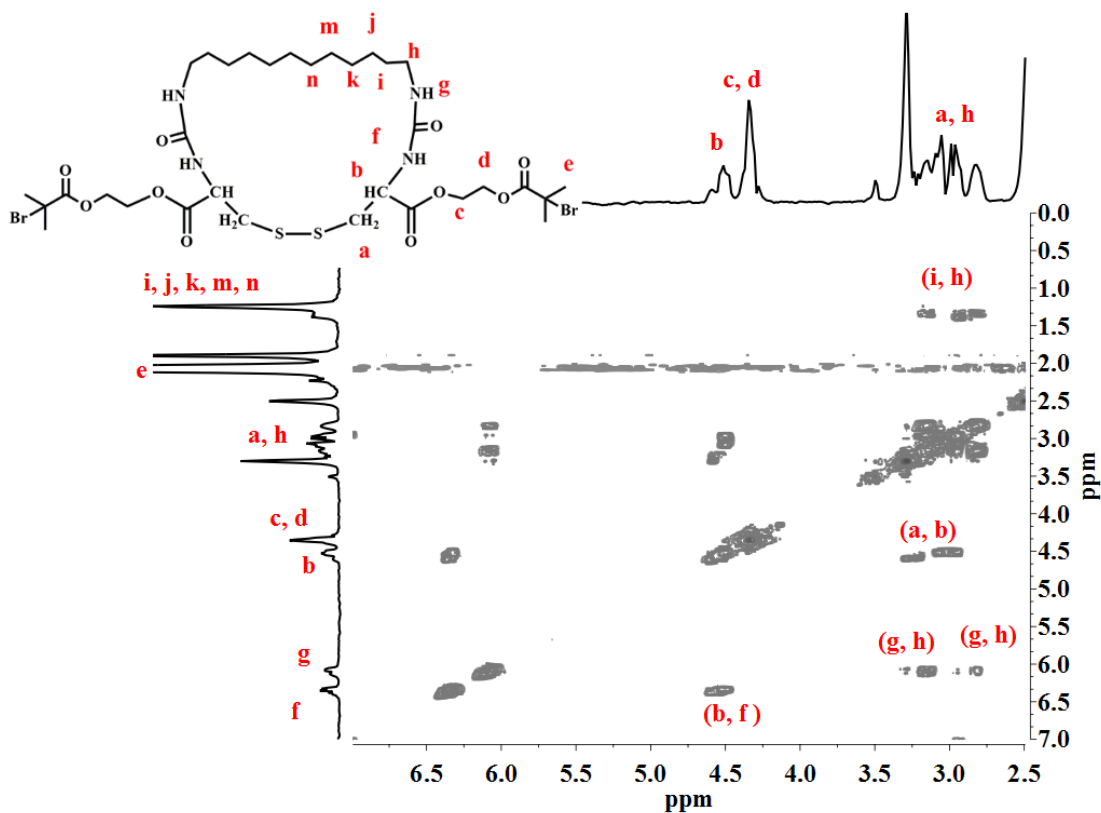


Figure S20. ^1H COSY spectrum of **6c** in $\text{DMSO-}d_6$

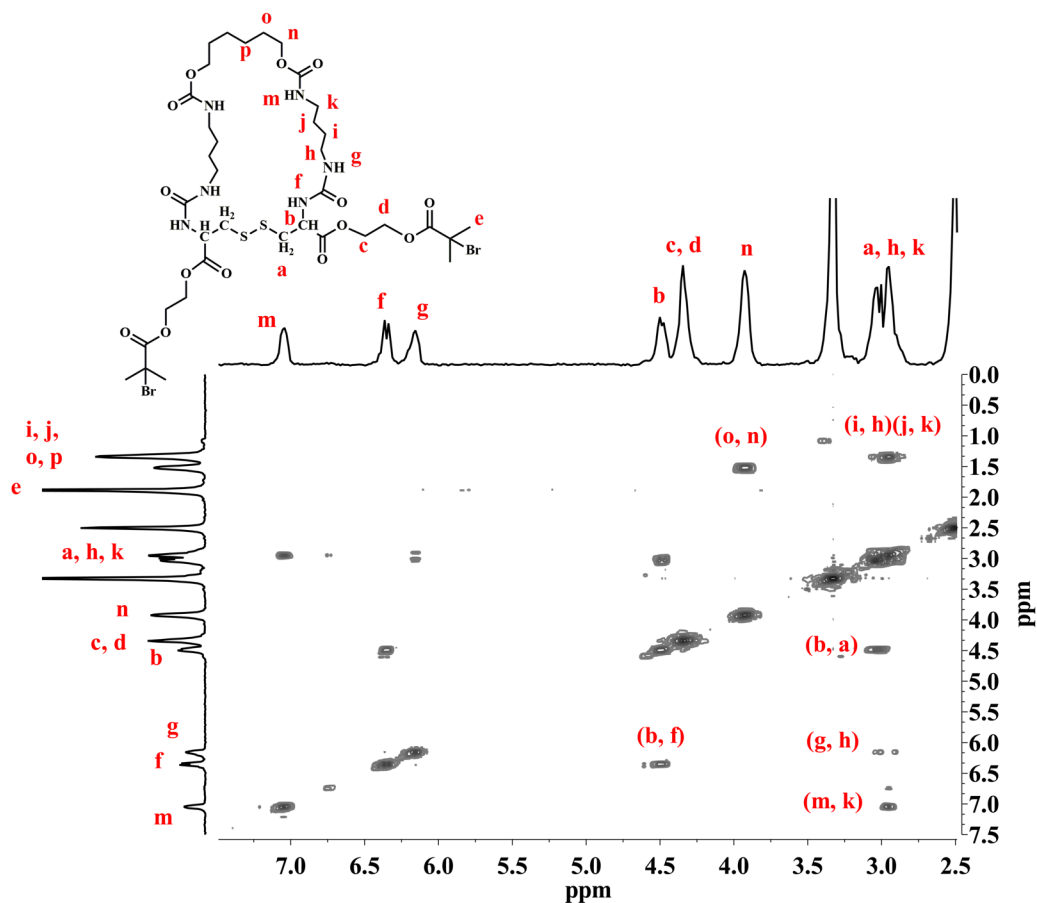


Figure S23. ^1H COSY spectrum of **6d** in $\text{DMSO-}d_6$

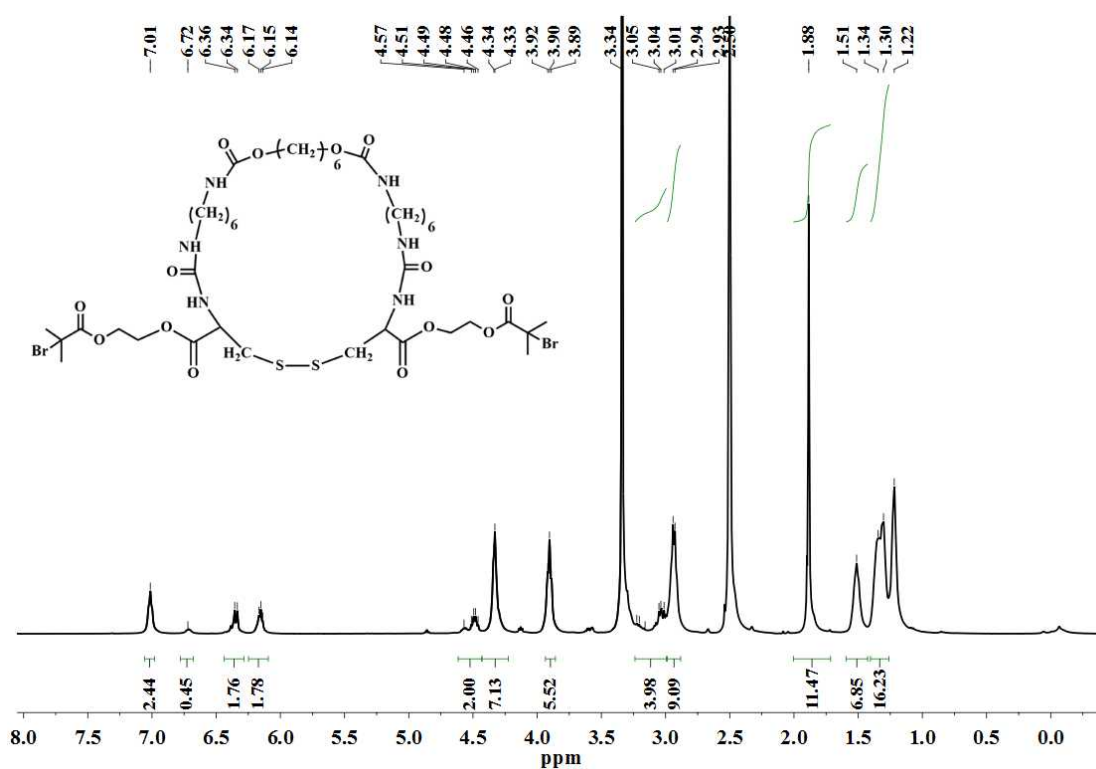


Figure S24. ^1H NMR of compound **6e** in $\text{DMSO-}d_6$.

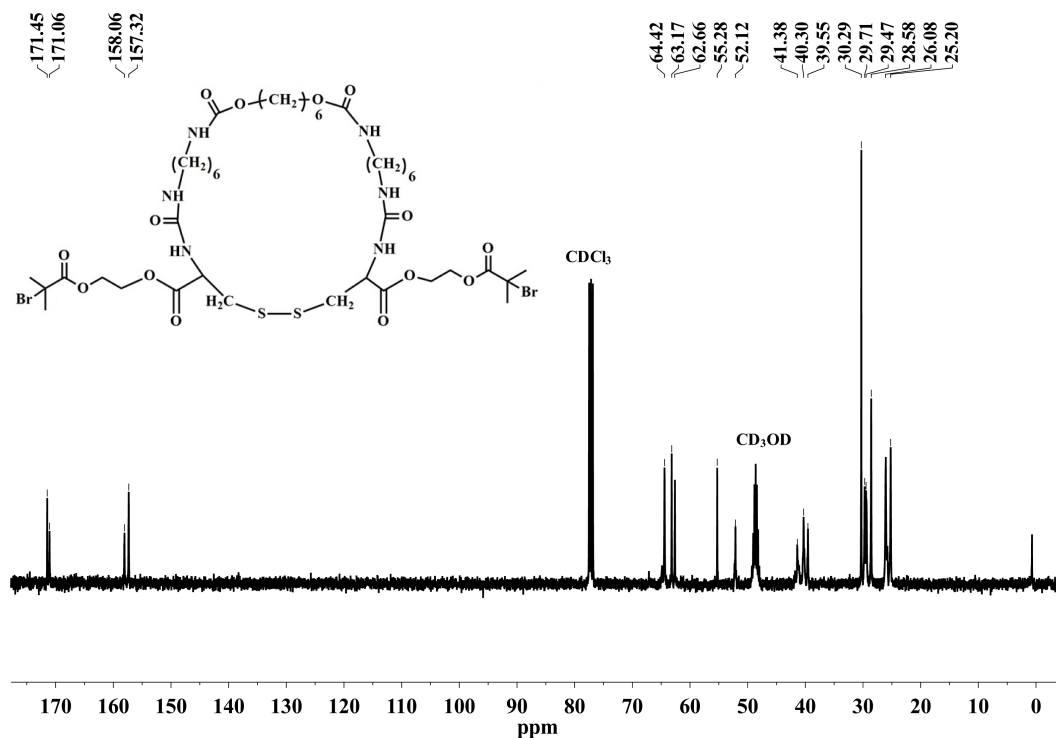


Figure S25. ^{13}C NMR of compound **6e** in $\text{CDCl}_3 + \text{CD}_3\text{OD}$.

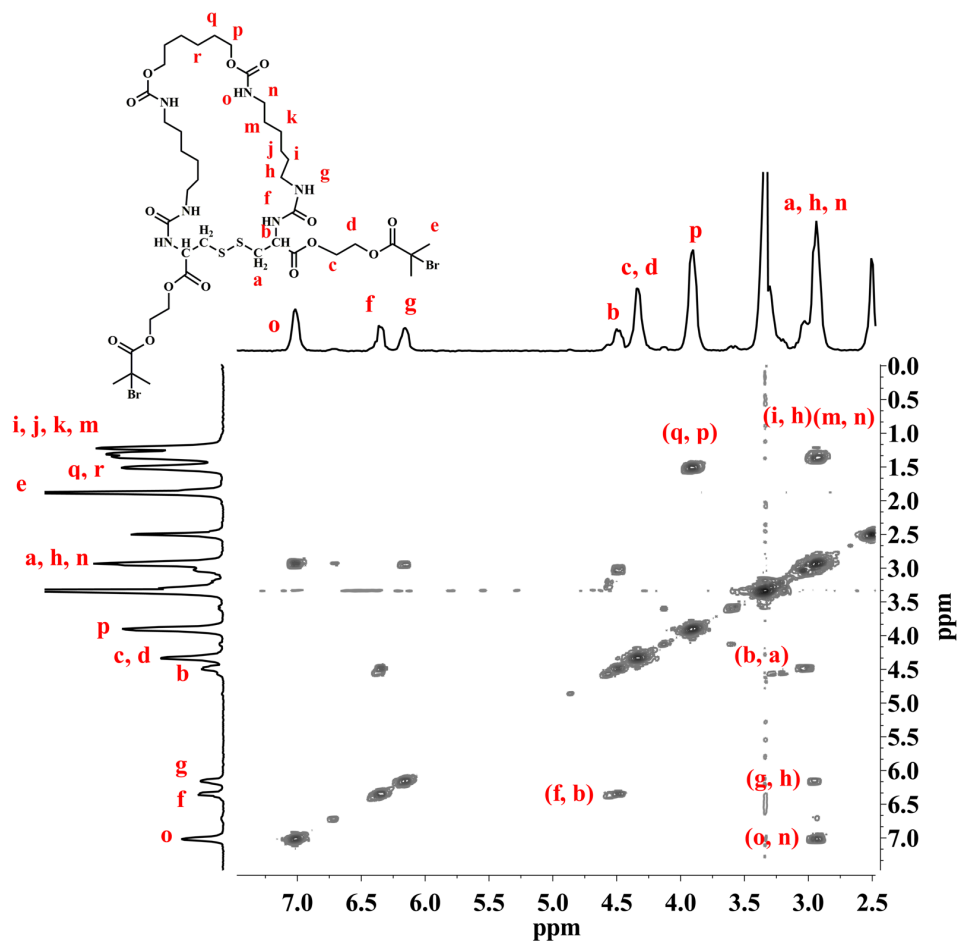


Figure S26. ^1H COSY spectrum of **6e** in $\text{DMSO-}d_6$

VI. Kinetic GPC curves

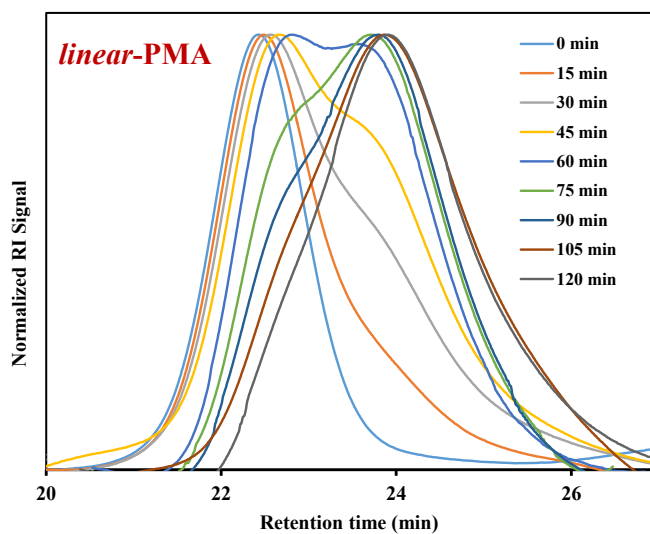


Figure S27. Evolution of GPC traces for sample *linear-PMA* upon sonication in THF.

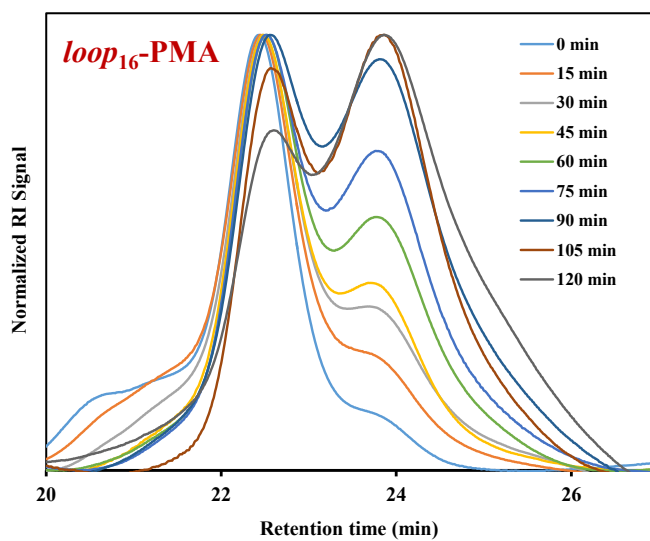


Figure S28. Evolution of GPC traces for sample *loop₁₆-PMA* upon sonication in THF.

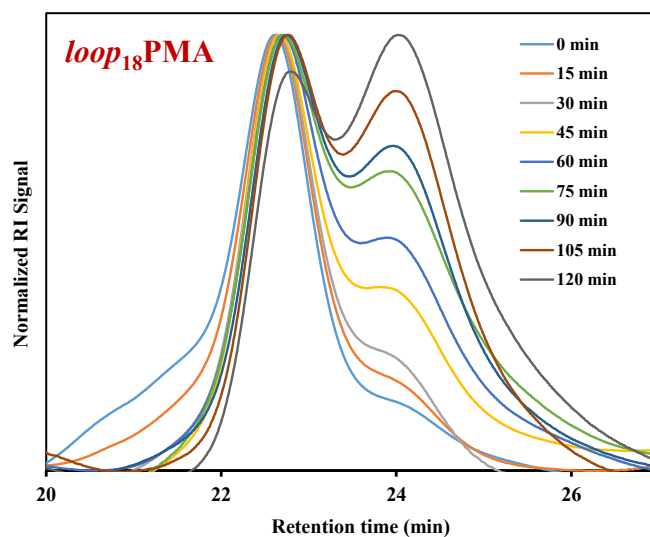


Figure S29. Evolution of GPC traces for sample *loop*₁₈-PMA upon sonication in THF.

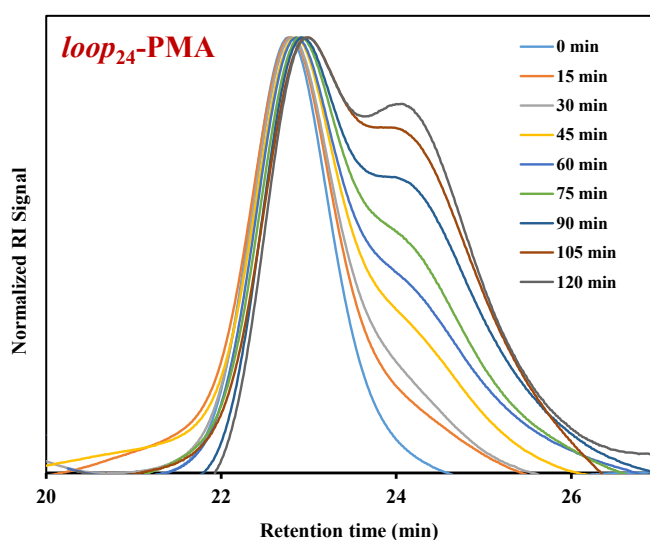


Figure S30. Evolution of GPC traces for sample *loop*₂₄-PMA upon sonication in THF.

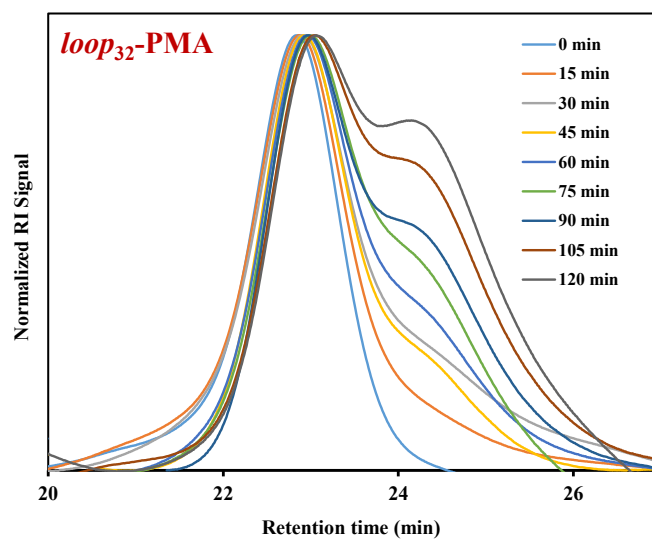


Figure S31. Evolution of GPC traces for sample *loop*₃₂-PMA upon sonication in THF.

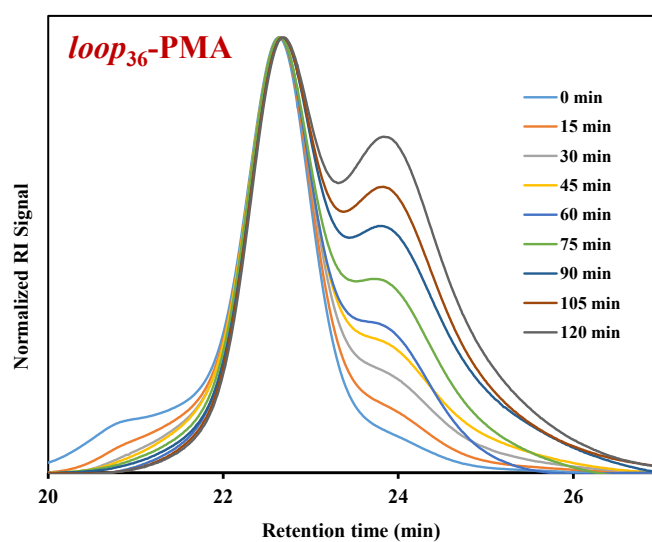


Figure S32. Evolution of GPC traces for sample *loop*₃₆-PMA upon sonication in THF.

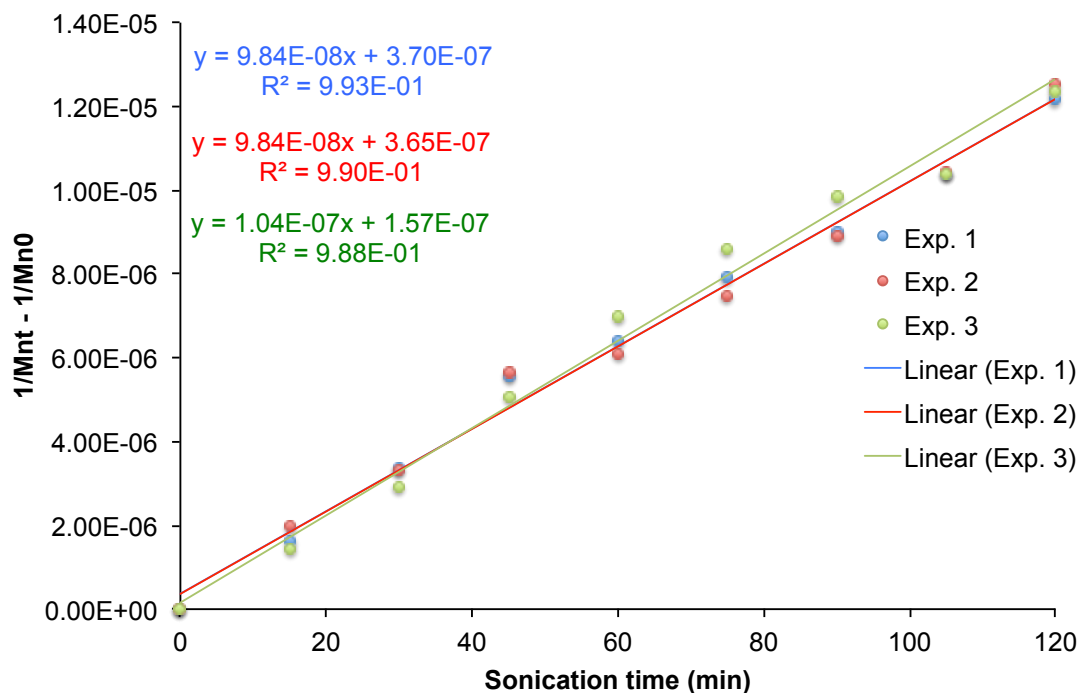


Figure S33. Plots of $1/M_{n,t} - 1/M_{n,0}$ as a function of sonication time and linear fits according to $1/M_{n,t} - 1/M_{n,0} = k't$ for *linear*-PMAs.

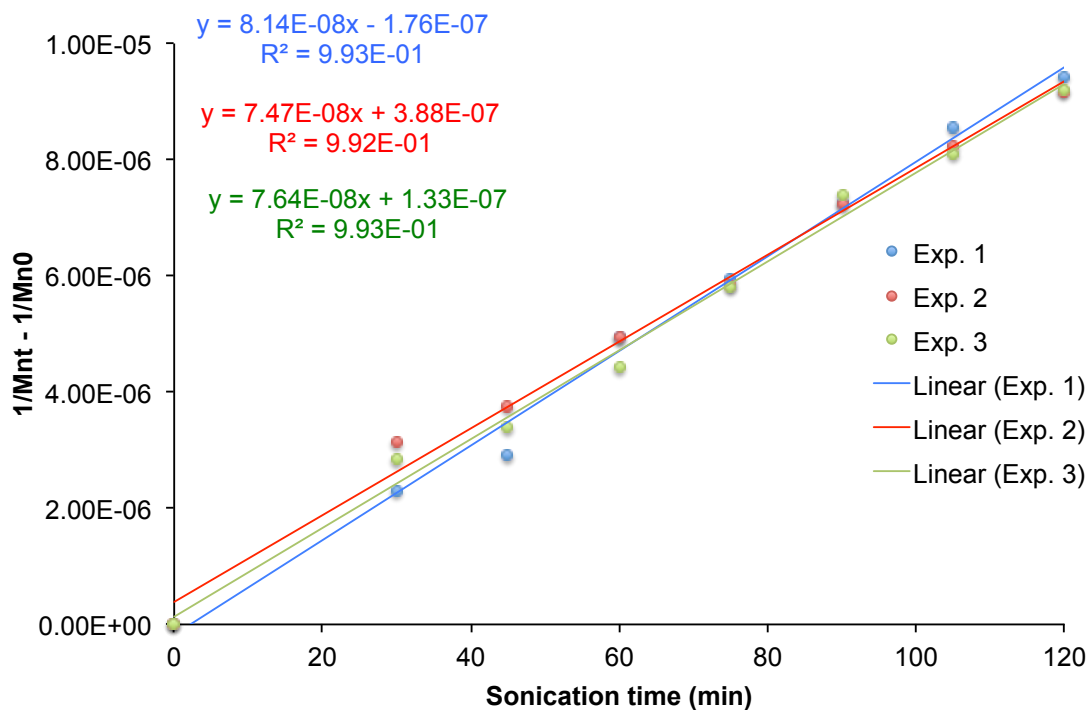


Figure S34. Plots of $1/M_{n,t} - 1/M_{n,0}$ as a function of sonication time and linear fits according to $1/M_{n,t} - 1/M_{n,0} = k't$ for *loop16*-PMAs.

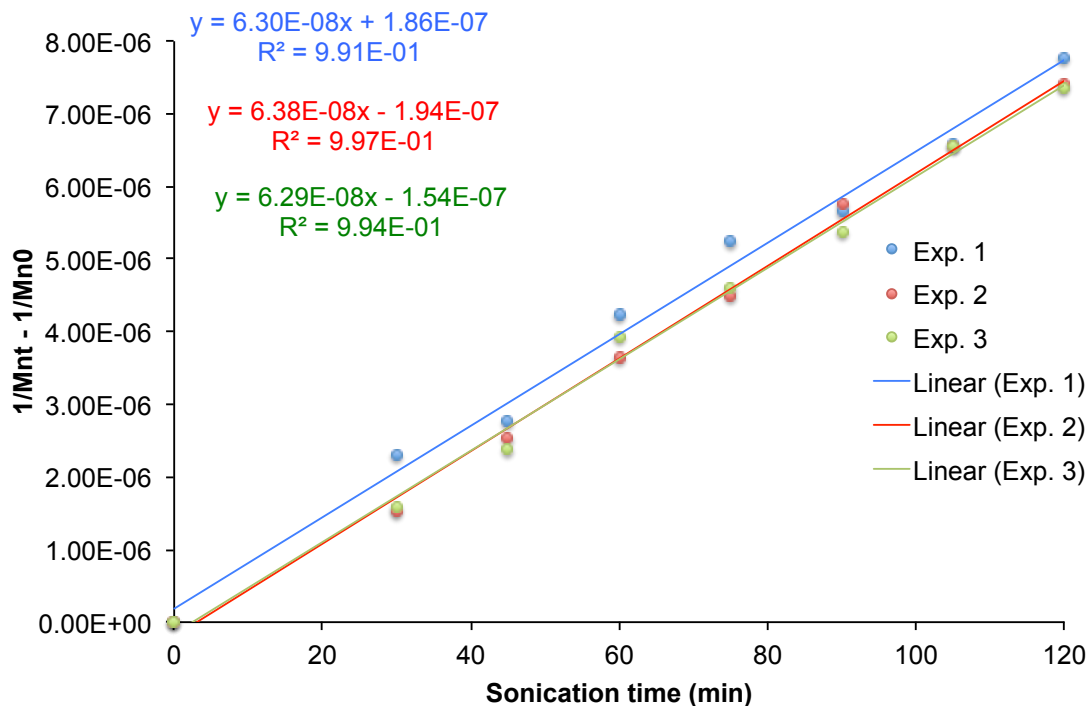


Figure S35. Plots of $1/M_{n,t} - 1/M_{n,0}$ as a function of sonication time and linear fits according to $1/M_{n,t} - 1/M_{n,0} = k't$ for *loop18*-PMAs

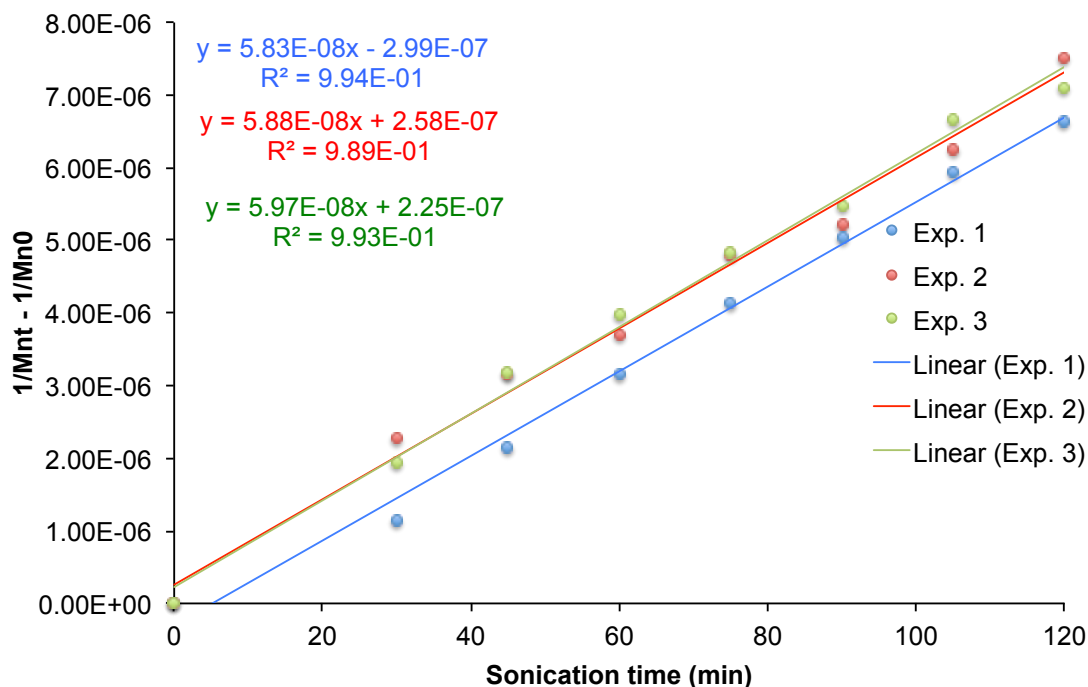


Figure S36. Plots of $1/M_{n,t} - 1/M_{n,0}$ as a function of sonication time and linear fits according to $1/M_{n,t} - 1/M_{n,0} = k't$ for *loop24*-PMAs

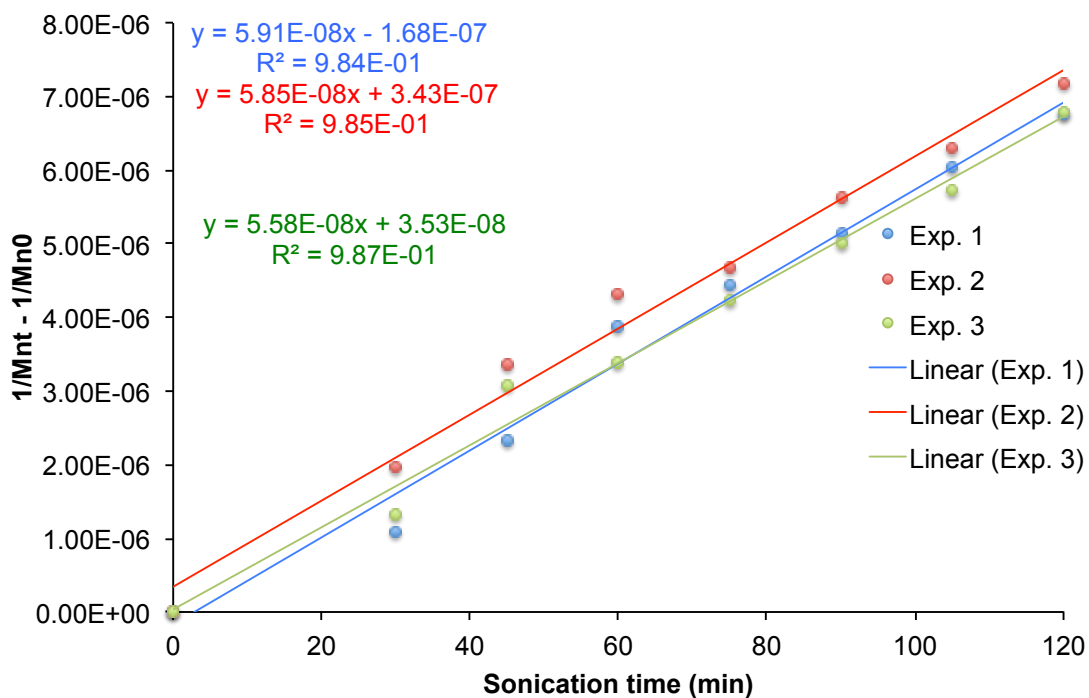


Figure S37. Plots of $1/M_{n,t} - 1/M_{n,0}$ as a function of sonication time and linear fits according to $1/M_{n,t} - 1/M_{n,0} = k't$ for *loop32*-PMA

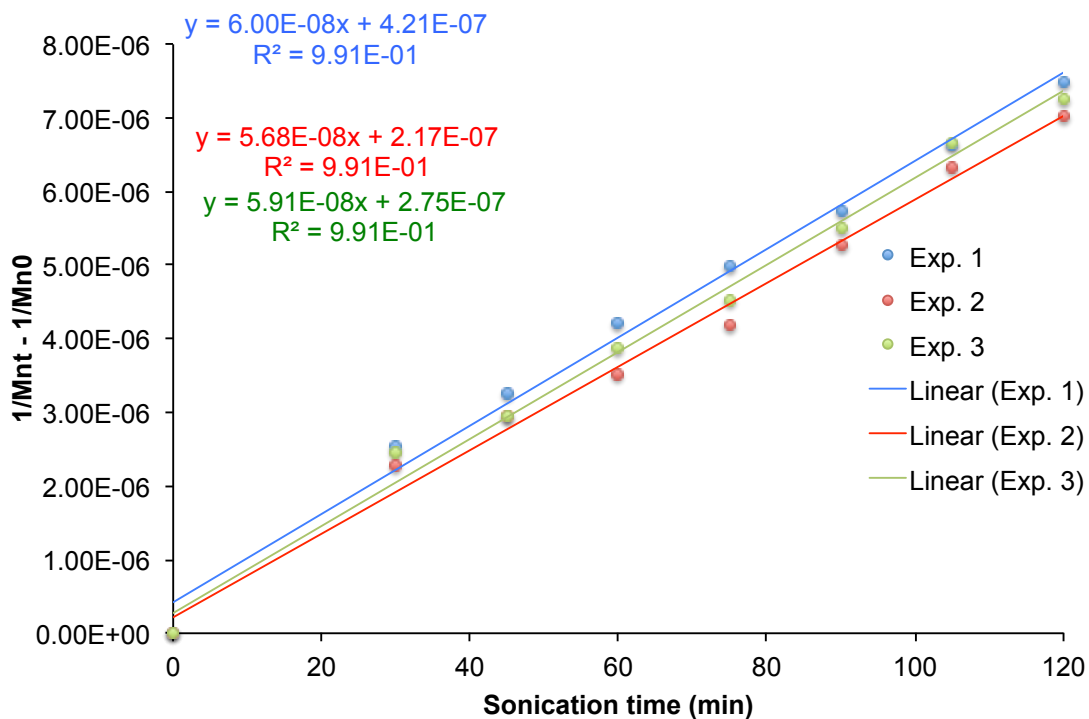


Figure S38. Plots of $1/M_{n,t} - 1/M_{n,0}$ as a function of sonication time and linear fits according to $1/M_{n,t} - 1/M_{n,0} = k't$ for *loop36*-PMA

Table S1. Rate constants k' calculated for all sonication experiments.

Sample	k'_1 ($\times 10^{-8}$ mol/g*min)	k'_2 ($\times 10^{-8}$ mol/g*min)	k'_3 ($\times 10^{-8}$ mol/g*min)	Average ($\times 10^{-8}$ mol/g*min)	Std. Dev. ($\times 10^{-8}$ mol/g*min)	k ($\times 10^{-6}$ min ⁻¹)	Std. Dev. ($\times 10^{-6}$ min ⁻¹)
<i>linear</i> -PMA	9.84 ± 0.32	9.84 ± 0.37	10.40 ± 0.43	10.03	0.32	8.63	0.28
<i>loop</i> ₁₆ -PMA	8.14 ± 0.28	7.47 ± 0.27	7.64 ± 0.27	7.75	0.35	6.67	0.30
<i>loop</i> ₁₈ -PMA	6.30 ± 0.25	6.38 ± 0.15	6.29 ± 0.15	6.32	0.05	5.44	0.04
<i>loop</i> ₂₄ -PMA	5.83 ± 0.19	5.88 ± 0.25	5.97 ± 0.21	5.89	0.07	5.07	0.06
<i>loop</i> ₃₂ -PMA	5.91 ± 0.31	5.85 ± 0.29	5.58 ± 0.26	5.78	0.17	4.97	0.15
<i>loop</i> ₃₆ -PMA	6.00 ± 0.24	5.68 ± 0.22	5.91 ± 0.22	5.88	0.16	5.06	0.14

VII. Statistical analysis

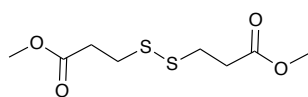
Statistical analysis was performed using a Student's t-test with a minimum confidence level of 0.1 for statistical significance and assuming equal sample sizes and unequal variance. All values are reported as the mean and standard deviation of the mean. The calculated values (using GraphPad Prism software) are listed in **Tables S2**, for all pairs of polymers. The standard deviation used in the t-test was the highest of the observed in the each of the three linear regressions or from the averaging of the k' .

Table S2. Student t test results comparing individual rate constants of every polymer pair in *gem*-DCC activation experiments. Red color indicates no significant difference between the pair.

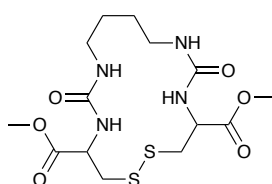
	<i>loop</i> ₁₆ -PMA	<i>loop</i> ₁₈ -PMA	<i>loop</i> ₂₄ -PMA	<i>loop</i> ₃₂ -PMA	<i>loop</i> ₃₆ -PMA
<i>linear</i> -PMA	0.0015	0.0001	0.0001	0.0001	0.0001
<i>loop</i> ₁₆ -PMA		0.0045	0.0017	0.0018	0.0013
<i>loop</i> ₁₈ -PMA			0.0943	0.0755	0.0735
<i>loop</i> ₂₄ -PMA				0.6388	0.8771
<i>loop</i> ₃₂ -PMA					0.7172

VIII. CoGEF Analysis

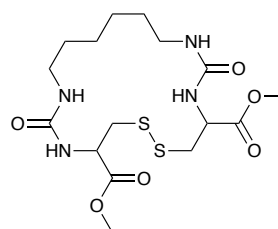
CoGEF calculations were performed on Spartan '14.⁶ Each macrocycle, taken as methyl esters, was minimized by DFT using the B3LYP/6-31G* level of theory. Then, the distance between the methyl carbons was increased in increments of 0.2 Å, followed by minimization and energy calculation (B3LYP/6-31G*) at each step. The energies were plotted against the energies. After disulfide bond scission, the calculations failed in a few steps, and therefore, were followed after addition of hydrogens to the thioradicals. F_{\max} values were determined from the slopes before each bond scission (H-bond, S-S and C-C). The model molecules that were used in this studies are the following:



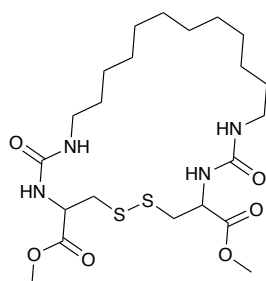
linear (S-S and C-C)



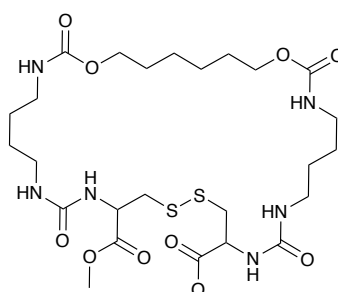
loop 16



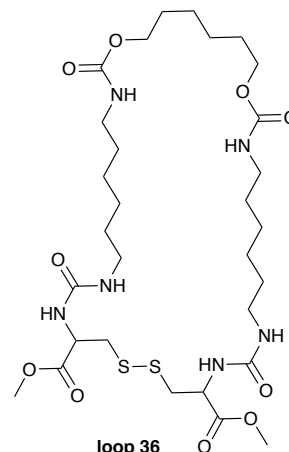
loop 18



loop 24



loop 32



loop 36

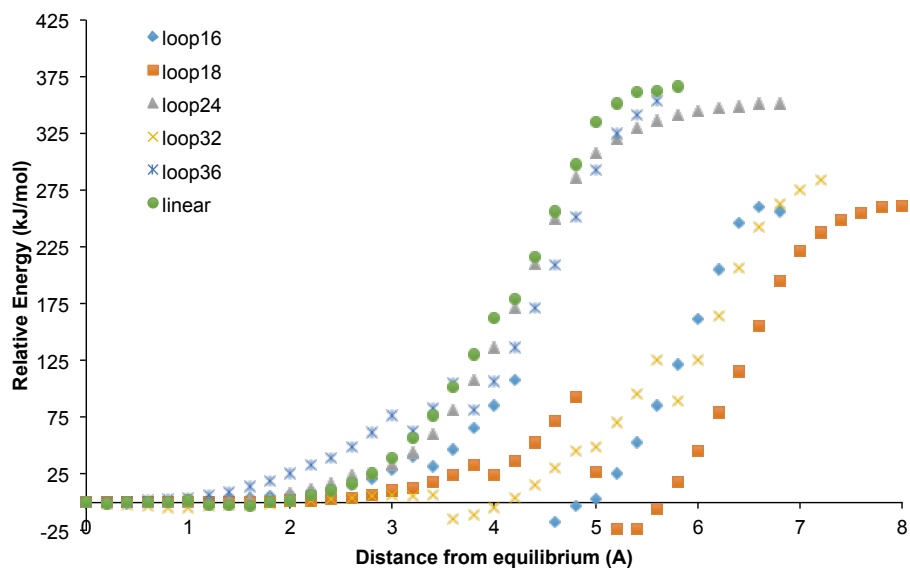


Figure S39. CoGEF for different macrocyclic models up to S-S bond scission.

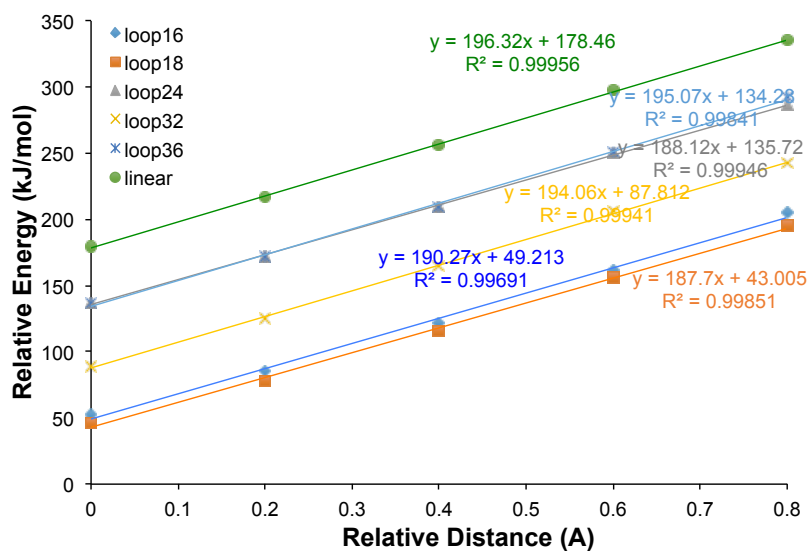


Figure S40. F_{\max} calculation in S-S bond scission.

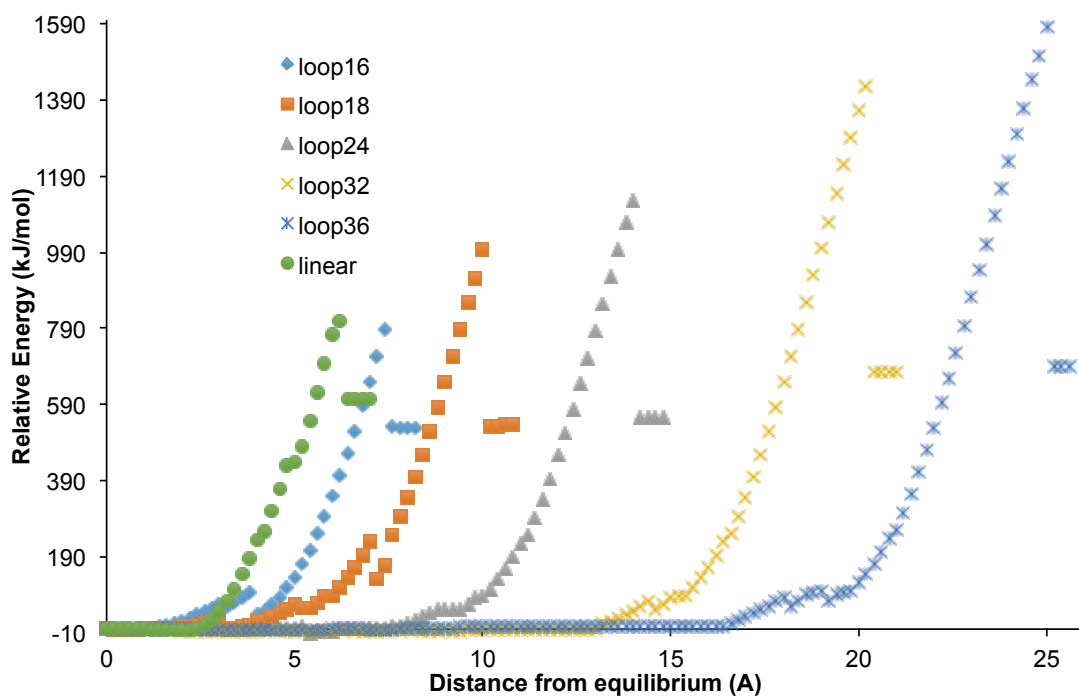


Figure S41. CoGEF for different macrocyclic models showing C-C bond scission.

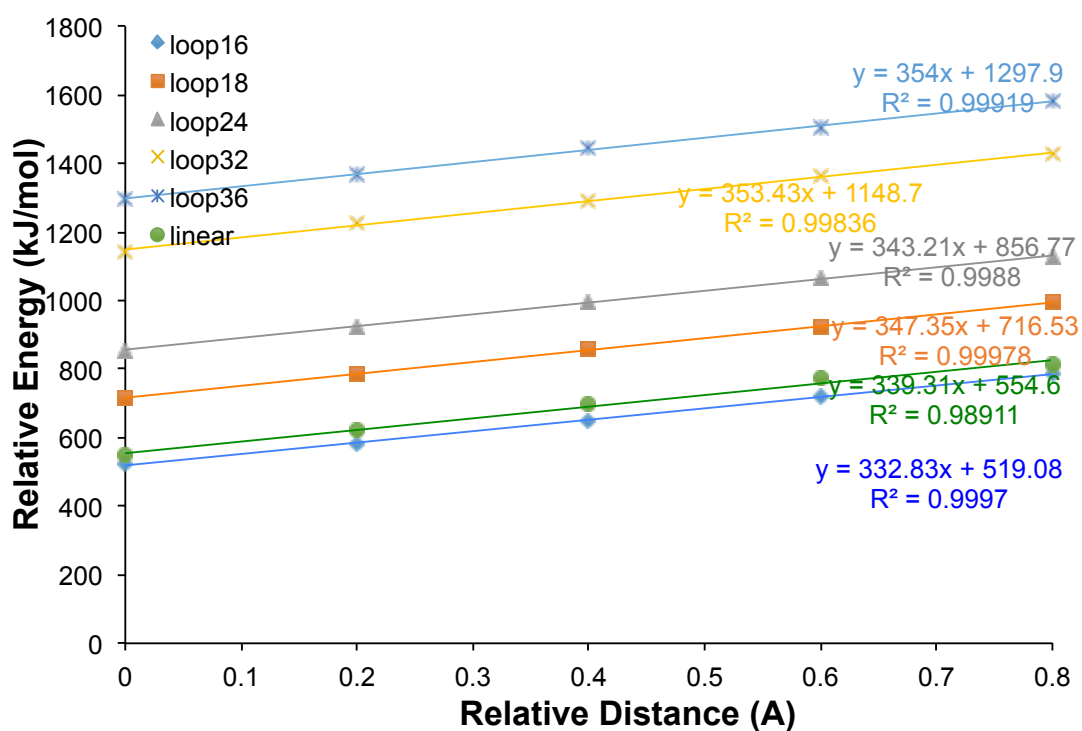


Figure S42. F_{\max} calculation in C-C bond scission (before conversion to nN unit).

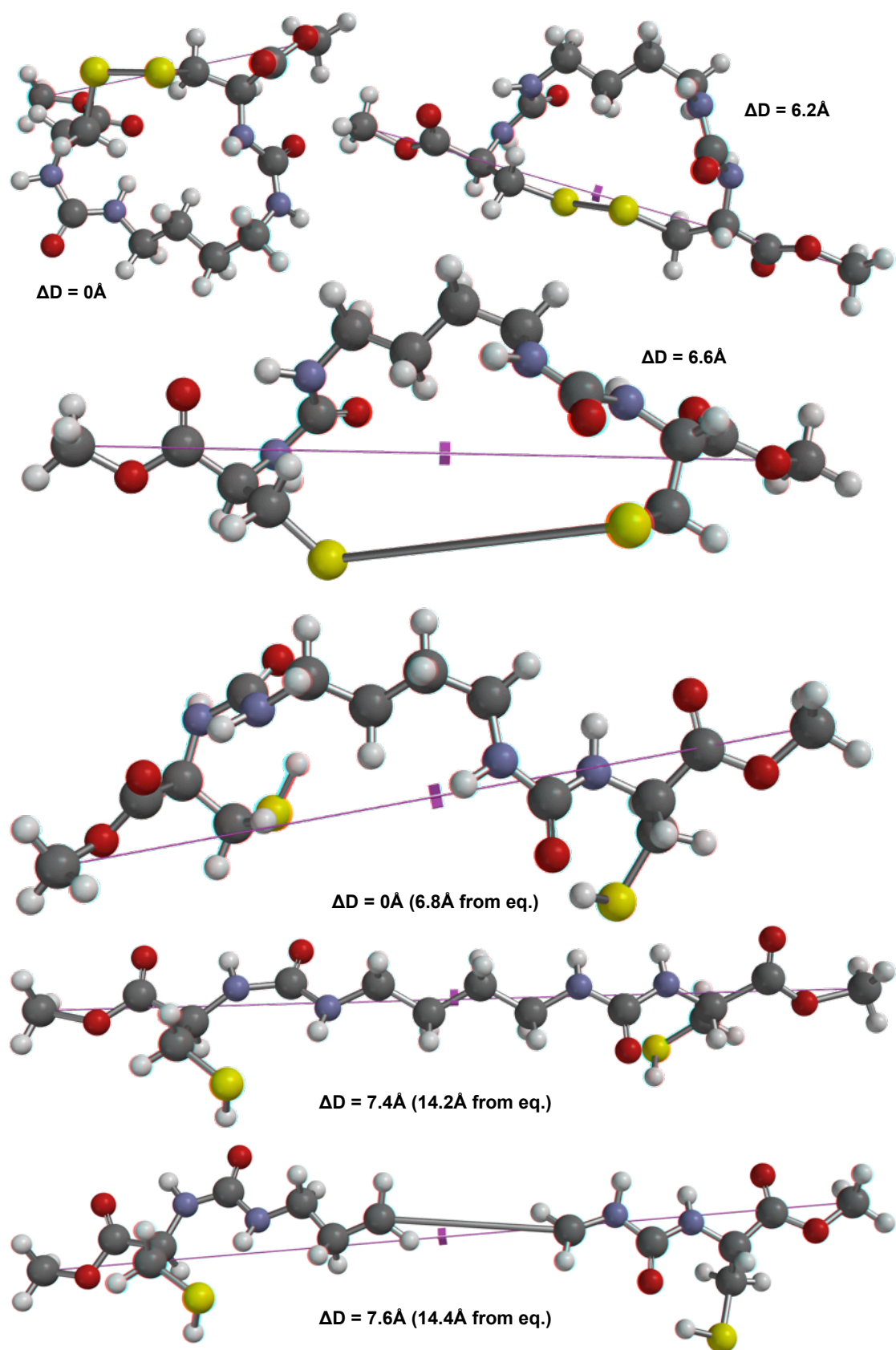


Figure S43. Structures from CoGEF for loop16 at equilibrium, before and after S-S bond scission; reduced after S-S bond scission, before and after C-C bond scission.

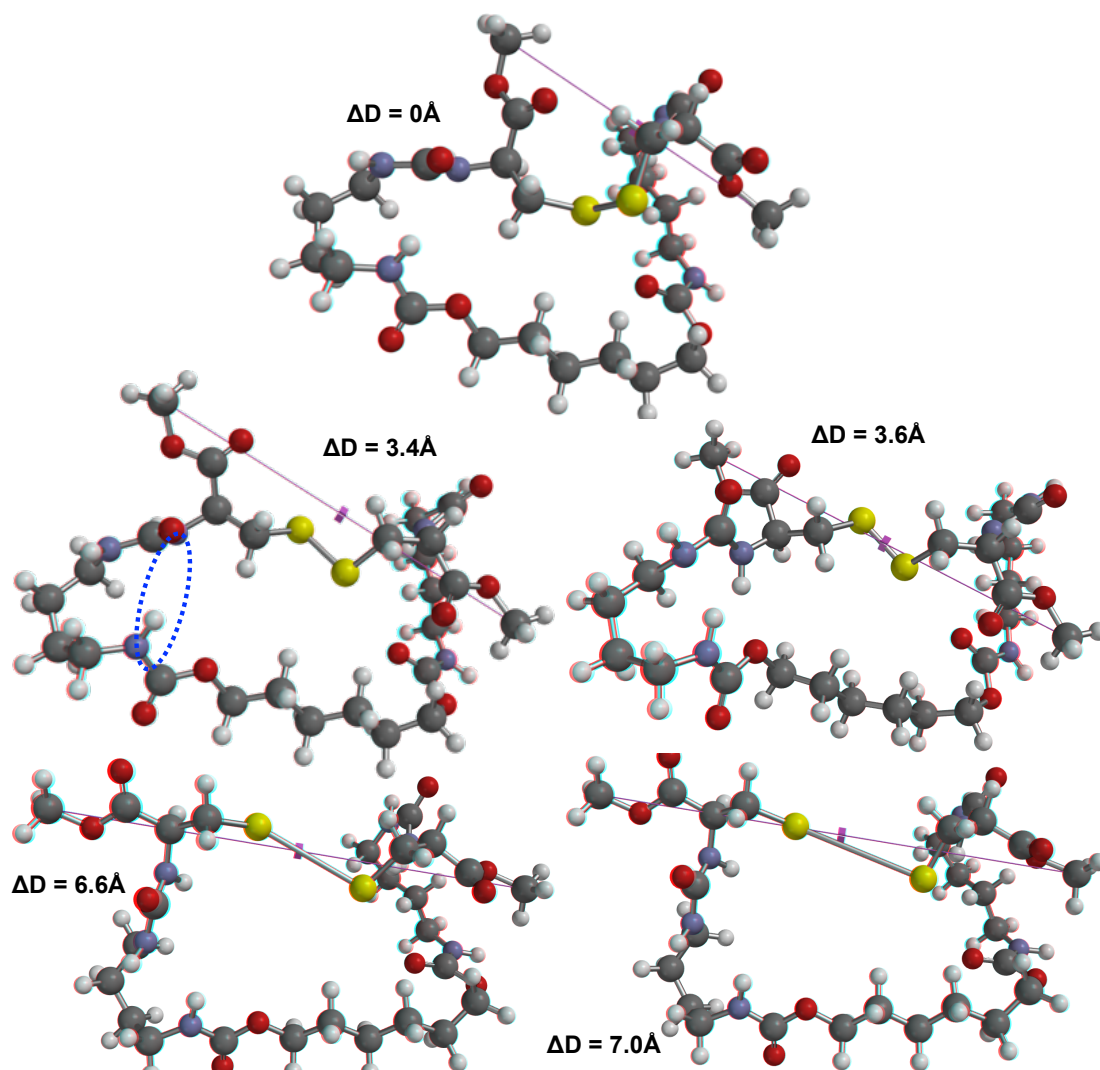


Figure S44. Structures from CoGEF for loop32 at equilibrium; before and after transannular H-bond scission (marked in blue); before and after S-S bond scission.

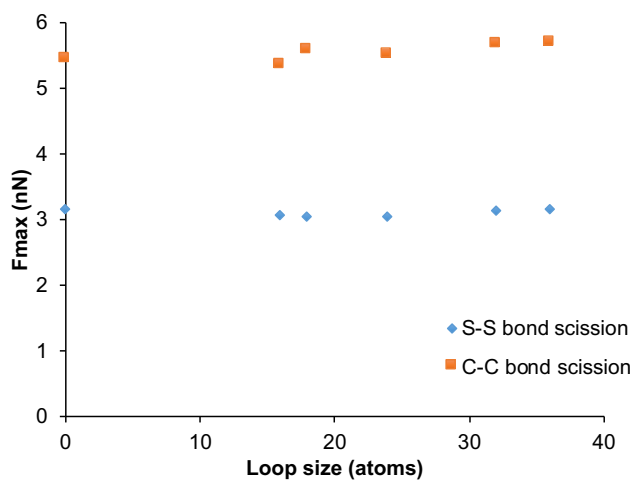


Figure S45. CoGEF (DFT) calculated force required for scission of S-S and C-C bonds in different loops and linear models.

IX. References

1. D. B. G. Williams and M. Lawton, *J. Org. Chem.*, 2010, **75**, 8351-8354.
2. Y. Zheng, Y. Guo, Y. Li, Y. Wu, L. Zhang and Z. Yang, *New J. Chem.*, 2014, **38**, 4952-4962.
3. J. Madsen, S. P. Armes, K. Bertal, H. Lomas, S. MacNeil and A. L. Lewis, *Biomacromolecules*, 2008, **9**, 2265-2275.
4. J. F. Tan, A. Blencowe, T. K. Goh, I. T. M. Dela Cruz and G. G. Qiao, *Macromolecules*, 2009, **42**, 4622-4631.
5. V. Percec, T. Guliashvili, J. S. Ladislaw, A. Wistrand, A. Stjerndahl, M. J. Sienkowska, M. J. Monteiro and S. Sahoo, *J. Am. Chem. Soc.*, 2006, **128**, 14156-14165.
6. M. J. Beyer, *Chem. Phys.*, 2000, **112**, 7307-7312